GEOLOGICAL SURVEY OF CANADA
OPEN FILE 7526

Micromorphological descriptions of till from pit K-62, Pine Point mining district, Northwest Territories

J.M. Rice, R.C. Paulen, J. Menzies, and M.B. McClenaghan

2014

Natural Resources Canada | Ressources naturelles Canada

Canada

GEOLOGICAL SURVEY OF CANADA
OPEN FILE 7526

Micromorphological descriptions of till from pit K-62, Pine Point mining district, Northwest Territories

J.M. Rice[1], R.C. Paulen[2], J. Menzies[1], and M.B. McClenaghan[2]

[1]Department of Earth Sciences, Brock University, St. Catharines, ON
[2]Geological Survey of Canada, Ottawa, ON

2014

doi:10.4095/293478

This publication is available for free download through GEOSCAN (http://geoscan.ess.nrcan.gc.ca/)

Recommended citation
Rice, J.M., Paulen, R.C., Menzies, J., and McClenaghan, M.B., 2014. Micromorphological descriptions of till from pit K-62, Pine Point mining district, Northwest Territories; Geological Survey of Canada, Open File 7526, 30 p. doi:10.4095/293478

Publications in this series have not been edited; they are released as submitted by the author.

Contribution to the Geological Survey of Canada's Geo-Mapping for Energy and Minerals (GEM) Program 2008-2013

TABLE OF CONTENTS

Abstract **1**

Introduction **1**

Location 1

Geology 1

Ice-flow history 2

Methods **3**

Field collection 3

Thin section production 3

Micromorphological analysis 5

Results **8**

Unit A 8

Sample 11-PTA-022 8

Sample 11-PTA-023B 9

Sample 11-PTA-023 10

Unit B 10

Sample 11-PTA-023A 10

Unit C 11

Sample 11-PTA-025 11

Sample 11-PTA-026 11

Sample 11-PTA-027 11

Sample 11-PTA-028 11

Sample 11-PTA-029 11

Sample 11-PTA-030 11

Sample 11-PTA-031 12

Sample 11-PTA-032 12

Sample 11-PTA-035 12

Sample 11-PTA-036 12

Unit D 12

Sample 11-PTA-037 12

Sample 11-PTA-038 12

Sample 11-PTA-040 12

Sample 11-PTA-041 12

Sample 11-PTA-042 12

Discussion **13**

Unit A 13

Unit B 13

Unit C 13

Unit D 14

Conclusions **13**

Acknowledgements **14**

References **14**

Appendix

Appendix A. Annotated thin sections and legend 17

Sample 11-PTA-022 17

Sample 11-PTA-023A 18
Sample 11-PTA-023B 18
Sample 11-PTA-025 19
Sample 11-PTA-026 19
Sample 11-PTA-027 20
Sample 11-PTA-028 20
Sample 11-PTA-029 21
Sample 11-PTA-030 21
Sample 11-PTA-031 22
Sample 11-PTA-032 22
Sample 11-PTA-035 23
Sample 11-PTA-036 23
Sample 11-PTA-037 24
Sample 11-PTA-038 24
Sample 11-PTA-040 25
Sample 11-PTA-041 25
Sample 11-PTA-042 26

Figures

Figure 1. Map showing the geological and geographical setting of the past-producing Pine Point mine district, Northwest Territories 2
Figure 2. Striation record identified on the shoulder of a pit in the Pine Point mining district 3
Figure 3. SPOT satellite image of Highway 5, southwest of Pine Point 3
Figure 4. Series of photographs illustrating the method followed during sample collection 4
Figure 5. Photograph of the north face of open pit K-62, showing four different till units (A to D) overlain by glacial Lake McConnell littoral sediments (Unit E)56
Figure 6. Series of photographs showing the method followed for preparing impregnated samples 6
Figure 7. Series of photographs showing steps followed for preparing thin sections 7
Figure 8. Flow chart describing the methodology used in thin section production 8
Figure 9. Chart showing the range of microstructures within the plasma and S-matrix of glacial sediments 9
Figure 10. Stratigraphy and lithofacies of the northern exposure at open pit K-62 10
Figure 11. Photographs of a thin section of sample 11-PTA-023, one of which has been annotated to highlight the contact between Unit A and Unit B 11

MICROMORPHOLOGICAL DESCRIPTIONS OF TILL FROM PIT K-62, PINE POINT MINING DISTRICT, NORTHWEST TERRITORIES

J.M. Rice[1], R.C. Paulen[2], J. Menzies[1], and M.B. McClenaghan[2]

[1]Department of Earth Sciences, Brock University, 500 Glenridge Avenue, St. Catharines, Ontario L2S 3A1
[2]Geological Survey of Canada, 601 Booth Street, Ottawa, Ontario K1A 0E8 (e-mail: bethmcclenaghan@nrcan-rncan.gc.ca)

ABSTRACT

A better understanding of glacial transport and depositional environments has resulted from micromorphological studies of glacial sediments over the last several decades. The past-producing Pb-Zn mine at Pine Point, Northwest Territories, has >20 m of continuous diamicton overlying low-relief Paleozoic bedrock, which provides a unique opportunity to further the investigation of micromorphology in the study of glacial sediments, in particular the sustained depositional record versus the erosional records of various ice-flow trajectories and how that information can help document indicator mineral dispersal. Pit-K62 at Pine Point has a ~23 m section of diamicton from which 19 samples were collected and thin sections prepared. This report describes sample collection, thin section production and analysis, and microstructure identification of each of these 19 samples. These results will be combined with glacial stratigraphy and indicator-mineral work previously completed for the area to refine exploration techniques for Mississippi Valley-type Pb-Zn deposits utilizing the transportation history of their indicator minerals.

INTRODUCTION

Micromorphology is a branch of soil sciences that uses low-magnification microscopy to examine micro-features found within unconsolidated sediments. Structures, patterns, arrangements of individual grains, and how they relate to each other microscopically can all help identify and characterize internal and external fields within englacial and subglacial sediments (Menzies et al., 2010). In contrast to conventional tools and methods used in glacial sedimentology, micromorphology allows for detailed examination of the relationships and patterns of sediment grains without destroying the sediment's texture. For this reason, interest and application of micromorphology has increased in the last several decades (e.g. van der Meer, 1987, 1993; Menzies and Maltman, 1992; Carr, 2001; Hiemstra and Rijsdijk, 2003; Baroni and Fasano, 2006; Larsen et al., 2007).

The Geological Survey of Canada (GSC), through Geo-mapping for Energy and Minerals (GEM) program (2008–2013), in collaboration with Brock University are investigating the applicability of micromorphology as an aid to traditional mineral exploration methods. A suite of glacial sediment samples from the past-producing Pine Point mining district has been collected to better understand how microscale investigations can assist in glacial drift prospecting. This open file will describe, in context of the defined glacial stratigraphy (Rice et al., 2013), the collection, preparation, and analysis of the micromorphological till samples and provide complete descriptions of these samples.

Geochemical data for the <0.063 mm fraction of the till samples from this study site have already been released (McClenaghan et al., 2012). Regional striation data have also been previously reported by Paulen et al. (2007), Oviatt et al. (2011), and Oviatt (2013). Glacial stratigraphy of the Pine Point region was described by Rice et al. (2013) using visual observations, clast fabrics, grain-size analysis, geochemical analysis, heavy-mineral concentrates, striation measurements, and pebble lithologies.

Location

The past-producing Pine Point Pb-Zn mine site is located on the southern shore of Great Slave Lake in the Northwest Territories (Fig. 1), approximately 800 km north of Edmonton, Alberta. The site is located ~50 km east-southeast of the town of Hay River and ~180 km south of Yellowknife. This area is part of the Great Slave Plain of the Interior Plains of western Canada (Bostock, 1970); and encompasses the Buffalo Lake topographic map sheet (NTS 85B). The region's Pb-Zn deposits are hosted within platformal carbonate rocks on the eastern edge of the Western Canada Sedimentary Basin (Hannigan, 2007). The Pine Point area has relatively low relief (less than 15 m), with a landscape dominated by black spruce peatland and discontinuous permafrost (Lemmen, 1990). Access to the former open pits is available by trucks and all-terrain vehicles, through the decommissioned roads and mine infrastructure.

Geology

The major Pine Point Pb-Zn orebodies are hosted within middle Devonian carbonate rocks that are located in, or are in close proximity to the dolomitized Presqu'ile barrier complex (Okulitch, 2006). The primary ore minerals are galena and sphalerite, which are the only minerals that occur at an economical level (Hannigan, 2007).

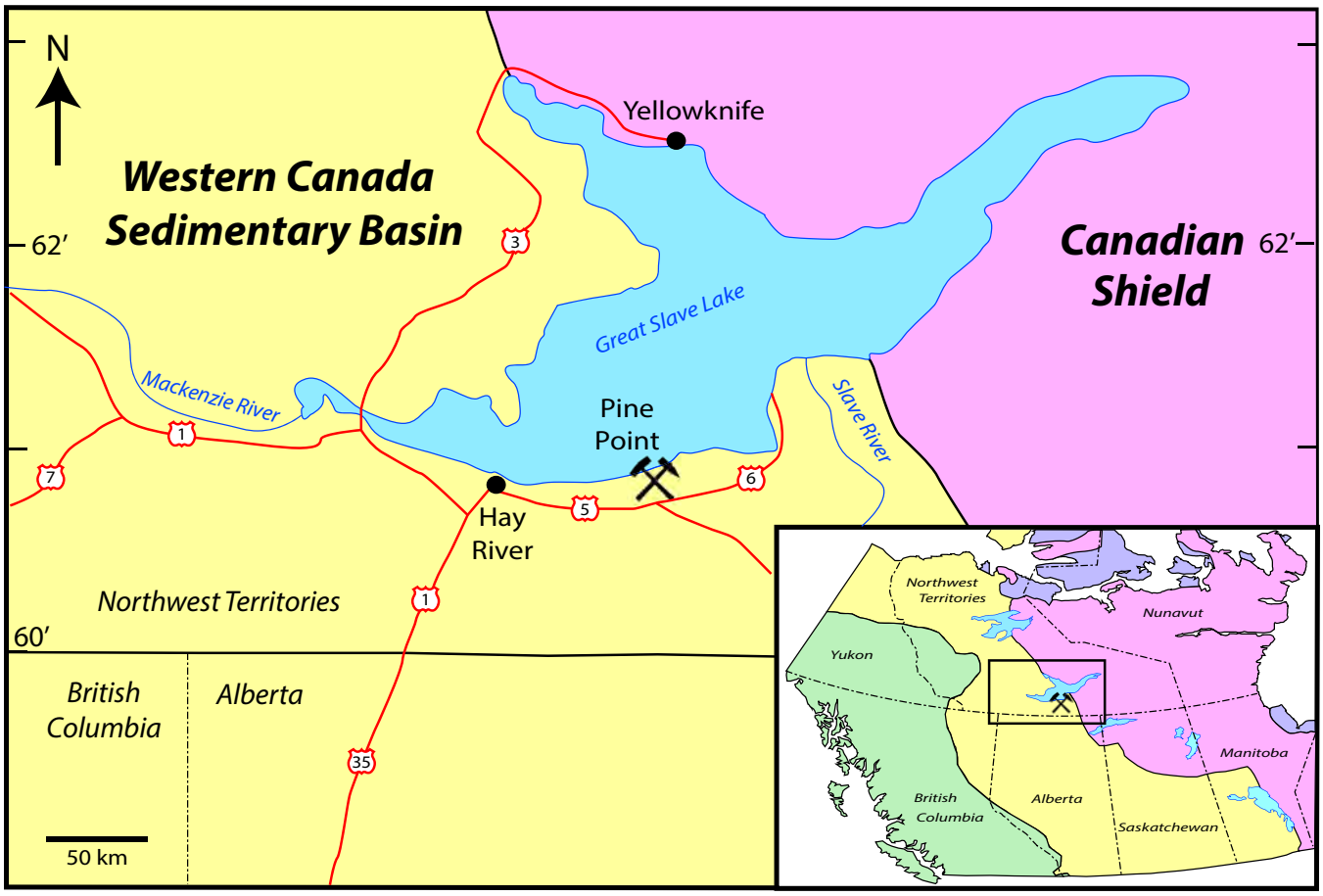

Figure 1. The geological and geographical setting of the past-producing Pine Point mine district, Northwest Territories. The study area is located at the eastern margin of the Western Canada Sedimentary Basin.

The Laurentide Ice Sheet (LIS) had a profound effect on the geomorphology of the Pine Point mining district, especially in terms of glacial-sediment deposition. The dominant glacial deposit was visually determined to be till (cf. Dreimanis, 1982), indicating that sediment had been transported and subsequently deposited by or from glacial ice with no or little sorting by water. The sediment matrix, which varies slightly throughout its entirety, usually consists of sandy silt with varying fissility and contains subrounded to subangular, faceted and striated clasts, ranging in size from granules to boulders. Regionally, the LIS deposited till to a thickness of greater than 20 m. Due to the gentle regional westward dip of the low-relief bedrock surface, the glacial sediments thicken westward from less than 1 m on the east side of the former mine property to more than 25 m in the westernmost open pits. Thicker sections of glacial sediment infill the bedrock karst-collapse structures. After the retreat of the LIS, the area was inundated by glacial Lake McConnell. Consequently, till surfaces were winnowed and a thin cover (<2 m) of beach and littoral glaciolacustrine deposits drape till and bedrock in the region (Lemmen et al., 1994).

Ice-Flow History

Surficial mapping was carried out in the Pine Point area by the GSC from 1989 to 1994, mainly to expand the knowledge of glacial Lake McConnell and related deposits (Lemmen, 1990; Lemmen et al., 1994). Small-scale surficial geology maps of the Klewi River (NTS 85A: Lemmen, 1998a) and Buffalo Lake (NTS 85-B: Lemmen, 1998b) identified a single phase of ice flow to the west. A more recent detailed surficial mapping of Breynat Point (NTS 85-B/15) was completed by Oviatt and Paulen (2013).

There is little published information on the ice-flow history of the region (Prest et al., 1968; Paulen et al., 2011), which is attributed to the lack of bedrock outcrop. Fieldwork conducted in 2010 by the GSC documented cross-striated bedrock surfaces on the shoulders (i.e. bedrock benches) of the exposed open pits (Oviatt et al., 2011; Oviatt, 2013). Striation measurements taken in the field (Fig. 2), combined with aerial-photo and satellite-imagery landform analysis, have determined a minimum of three ice-flow trajectories (Fig. 3). The earliest flow was to the southwest (~230º). An intermediate flow to the northwest (~300º) and a later westward-southwestward (~250º) flow were also

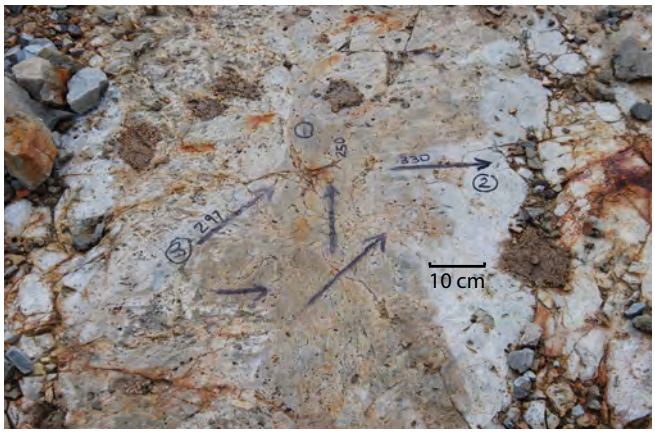

Figure 2. Striation record identified by Oviatt et al. (2011) on the shoulder of a pit in the Pine Point mining district showing three striation records. The youngest (1) is towards the west-southwest, a middle record (2) is to the northwest, and the latest recorded striation (3) to west-northwest.

identified. A single striation record also hints at a possible short-lived flow toward the northwest (~330º). The crosscutting relationships indicate that this phase must have occurred before the intermediate northwestward (~300º), and later westward-southwestward (~250º) phases. Landforms in the region are streamlined parallel to the last phase (~250º) of ice-flow direction (Fig. 2), re-shaping older oriented landforms that were formed during the intermediate (~300º) glacial event.

METHODS

Field Collection

Thin section analysis first required the collection of undisturbed, oriented, bulk till samples. Multiple methods were employed to collect samples in the field, all following the general outline of van der Meer (1996). First, existing talus and loose debris was removed to reveal in situ glacial sediment (Fig. 4A). After removing the lid (Fig. 4B), a Kubiëna tin is inserted into the sediment. A knife was used to clear space for the tin to enter the face (Fig. 4C), while making sure not to force the tin and disturb the sediment (Fig. 4D). Azimuth, up (vertical) direction, sample number, and front of the sample were recorded. When field conditions, such as fissility, hardness, and/or clast content, did not allow for the use of Kubiëna tins, chunks of sediment were carefully etched out and removed from the face. If after removing the Kubiëna tin it is not completely filled with diamict, sand (which is easily identified later in thin section) was added to pack the sample and prevent disturbance during transport (Fig. 4E). Filled Kubiëna tins or chunk samples were then individually placed in separate plastic bags, wrapped in tape, and transported back to field camp to be vacuum-sealed to keep the moisture in the

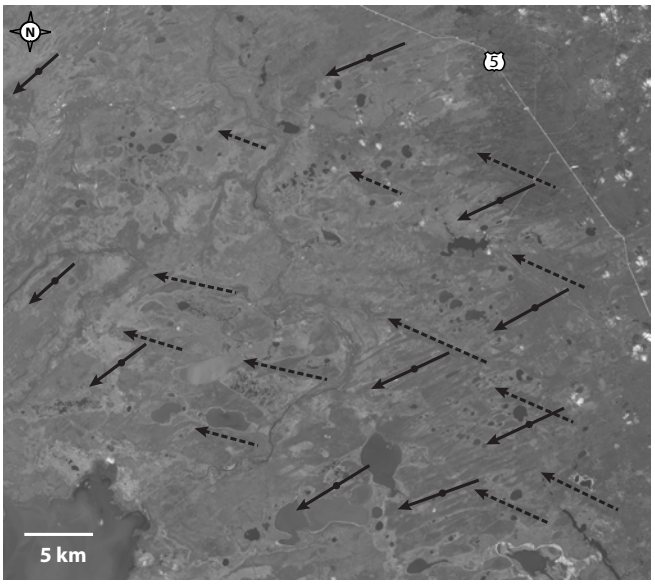

Figure 3. SPOT satellite image of Highway 5, southwest of Pine Point (see Fig. 1), showing the older, large northwest-trending glacial landforms (dashed arrows) crosscut by finer southwest-trending flutings (solid arrow) from the last glacial event (cf. Rice et al., 2013).

bag and improve durability (Fig. 4F). The samples were then packed and shipped for processing.

To ensure adequate sampling of each identified unit, sample locations for micromorphological investigation were determined from field observations (see Fig. 5; Rice et al., 2013). A minimum of one micromorphological sample was collected from each identified unit, with additional samples being collected at ~ 0.5 m vertical increments within the same unit and across visible contacts. Care was taken not to collect samples in close proximity to large cobbles or boulders, as these may have locally influenced structures within the sediment and thus the sample would not accurately reflect the true dynamic of the diamict (Boulton, 1976).

Thin Section Production

Sample preparation and thin section production was carried out at the Brock University Petrography Thin-sectioning Laboratory. Production of thin sections followed the steps and techniques outlined by Fitzpatrick (1984), Murphy (1986), Lee and Kemp (1993), van der Meer (1993), Carr and Lee (1998), and Menzies (2000). Once received, samples were unwrapped and checked for any damage that may have occurred during shipping. Undamaged samples were air dried for approximately 2 to 3 weeks. Samples, with sample number and orientation marked (Fig. 6A), were then wrapped in aluminum foil. The foil wrap was then perforated (Fig. 6B) to allow resin to completely surround the sediment. A resin bath was prepared by placing a plastic lining into a cardboard box (Fig. 6C). Samples were placed into the box and enough resin was added

Figure 4. Series of photographs illustrating the method followed during sample collection. **(A)** The in situ diamicton was exposed. **(B)** An empty Kubiëna tin with both ends removed (75 mm x 55 mm x 40 mm). **(C)** Kubiëna tin was inserted into the diamict using a till knife to ease its entry. **(D)** A completely inserted Kubiëna tin just before removal; the surrounding diamict was removed to allow the sample to be cut out. (**E)** An incompletely filled Kubiëna tin was packed with well sorted sand to ensure the sample was not disturbed in transport. **(F)** Samples were vacuum-sealed prior to shipment and processing.

to completely submerge them (Fig. 6D). The resin was a blend of acetone and Ecopoxy©— an organic-based hardening solvent—and was combined manually with a rubber policeman until completely mixed (~5 mins). After hand mixing, the solution was placed on a magnetic stirring plate for an additional 5 minutes.

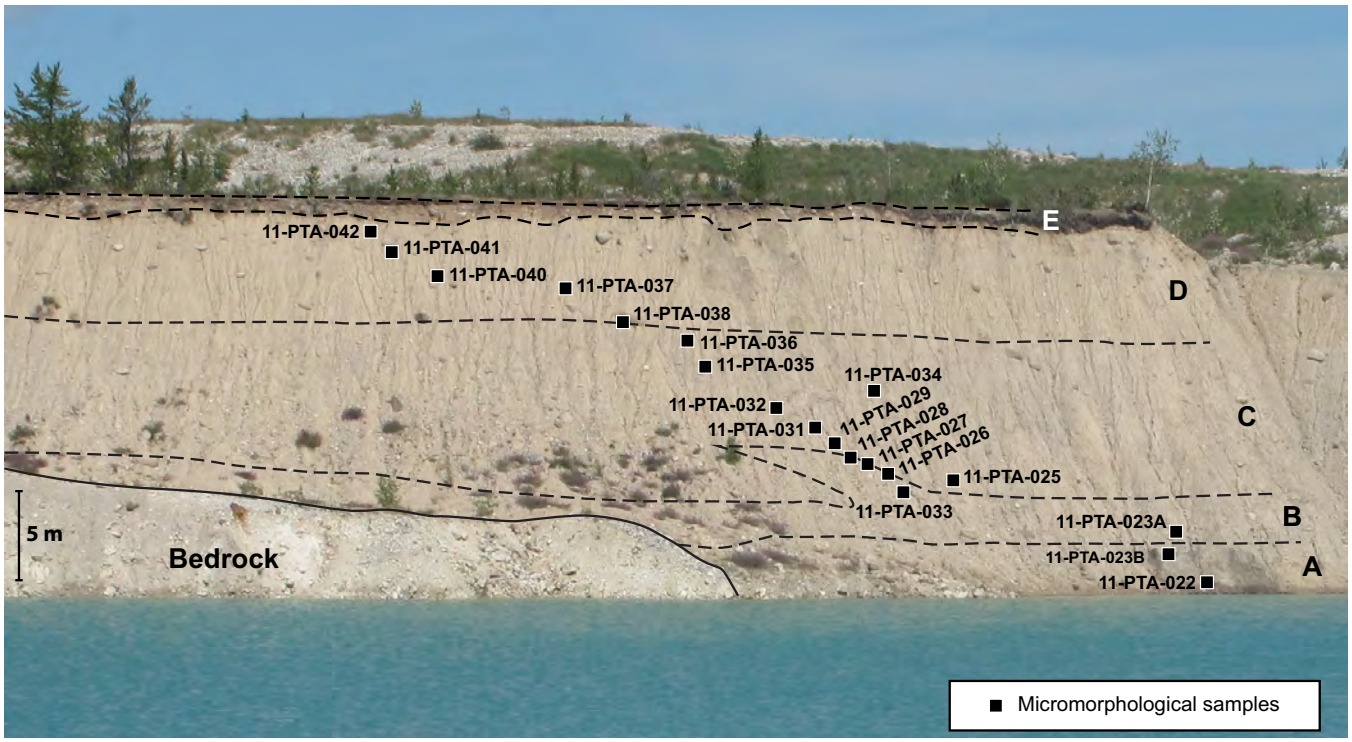

Figure 5. North face of open pit K-62, with four different till units (A to D) overlain by glacial Lake McConnell littoral sediments (Unit E). Total height of the section is 23 m. Dashed lines indicate the approximate till contacts. Sample locations and labels are indicated.

Additional Ecopoxy© slow hardener was added and mixed for an additional 30 minutes.

Over consolidation and stress experienced by most glacial sediments results in poor porosity and permeability, making resin impregnation difficult. Transport of resin through the sample requires grain-to-grain translocation of the fluid through the sediment, often leaving the central portion of the slide without full impregnation (cf. Carr and Lee, 1998). High clay content in samples also reduces the permeability, leading to uneven resin distribution. Immersed samples were allowed to impregnate for ~1 week in a vacuum chamber (at 12–17 kg/cm). Hydrophobic acetone acted to drive out all moisture within the sediment, allowing it to be replaced with resin.

The resin bath was checked daily and topped up with additional resin when needed. Once the samples were impregnated (Fig. 6E), excess resin was broken off by hand (Fig. 6F) and the samples were cured for another 4 to 5 days in a sparkless lab oven at 40–45ºC, after which they were cooled in a fume hood for 24 hours. The solidified samples were cut in half using a Servocut®-M250 (Fig. 6G) and analyzed for successful resin penetration (Fig. 6H). If needed, surface impregnation was applied to the sample to ensure cohesion of the material during the mounting process. Subsequently, solidified samples were mounted and a block ~1 cm thick was cut (Fig 7A,B; cf. Kemp, 1985; Lee and Kemp, 1993; Carr and Lee, 1998; van der Meer and Menzies, 2006) This small block was then ground down (Fig. 7C) and polished using a PM 2A® polisher and subsequently mounted on a glass plate (75 mm x 50 mm x 1 mm) that had been etched with the sample number and up direction. Once reduced to a reasonable thickness, the block is hand-ground using a Petro-Thin® machine (Fig. 7D) to a thickness of ~30 µm (Fig. 7E). The thin sections were then analyzed under a microscope to determine if the thickness of the sample was acceptable or whether further grinding was required. Once the thin section was cleaned and a cover slip added (Fig. 7F), it was ready for microscopic examination (Fig. 7G). This methodology has summarized in the flow chart shown in Figure 8.

Micromorphological Analysis

Analyses of thin sections collected from Pit-K62 were completed at low magnification (6.5-10X) in plain light using a Wild-Heerbrugg® M420 microscope, affixed with a Nikon® Digital sight DS-Fi1 digital imaging device. Samples were macroscopically examined with the naked eye and visible structures, range of grain size, and grain distribution were noted. Nikon® NIS-Br imaging software was then used to measure grain orientation, grain length, sphericity of grains, and also to identify texturally different areas within the plasma. This software was also utilized to stitch together individual images to create a large composite of the slide. Images of the composite slides were

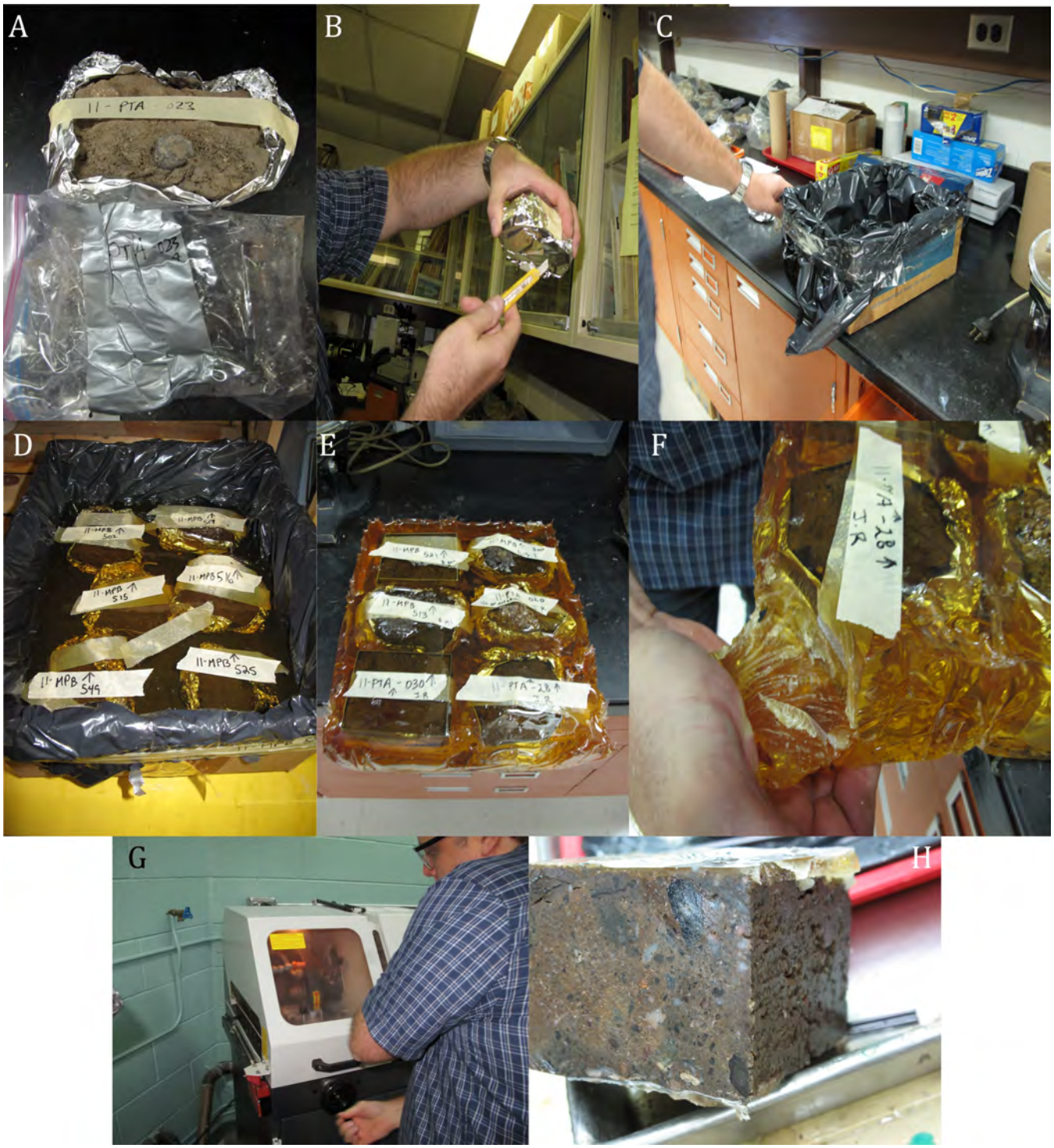

Figure 6. Series of photographs showing the method followed for preparing impregnated samples. **(A)** Samples, which were received vacuum-sealed in plastic bags, were removed and wrapped in tin foil, leaving the top open. **(B)** The bottom of the tin foil wrap was perforated to allow the flow of resin around the sample. **(C)** A plastic bag was placed around a cardboard box, which was used for impregnating the samples. **(D)** Samples were submerged in resin and allowed to cure for 2 weeks. **(E)** The **s**amples were cured in a vacuum hood for 2 weeks. **(F)** The excess resin was removed from samples. **(G)** The samples were then cut into manageable blocks. **(H)** The final result was a block of impregnated sample.

printed in high quality and a comprehensive microscopic analysis was completed with an initial focus on size range, distribution, shape, and general lithology of the skeletal grains. This was followed by a systematic analysis of the structures, starting from the upper right-hand corner of the thin section and working in a snake-like fashion to the end of the slide, noting any voids (orientation, type, and distribution) or other micro-

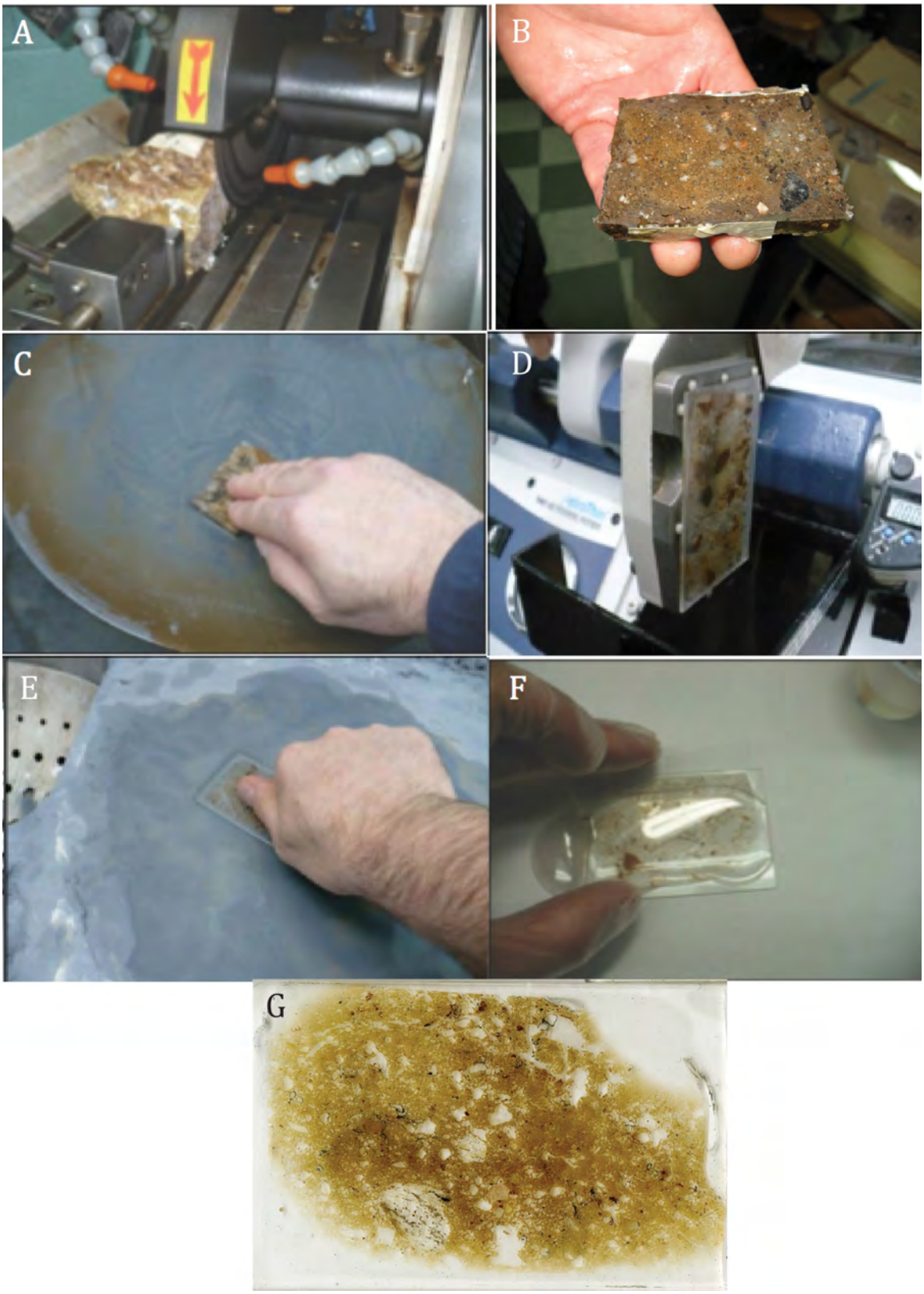

Figure 7. Series of photographs showing the steps that were followed for thin section prepation. **(A)** The larger solidified sample was cut down into ~1 cm thick slabs. **(B)** The **r**esulting block was cut and trimmed to thin section dimensions. **(C)** The sample was ground down on a lap wheel and then mounted on a glass slide. **(D)** The thin section was mechanically ground down to ~35 µm. **(E)** The sample, which had been further ground down by hand to ~30 µm, was inspected under a low-magnification microscope to ensure ideal thickness. **(F)** A cover slip was added to the finished thin section. **(G)** The resulting scan of a finished thin section.

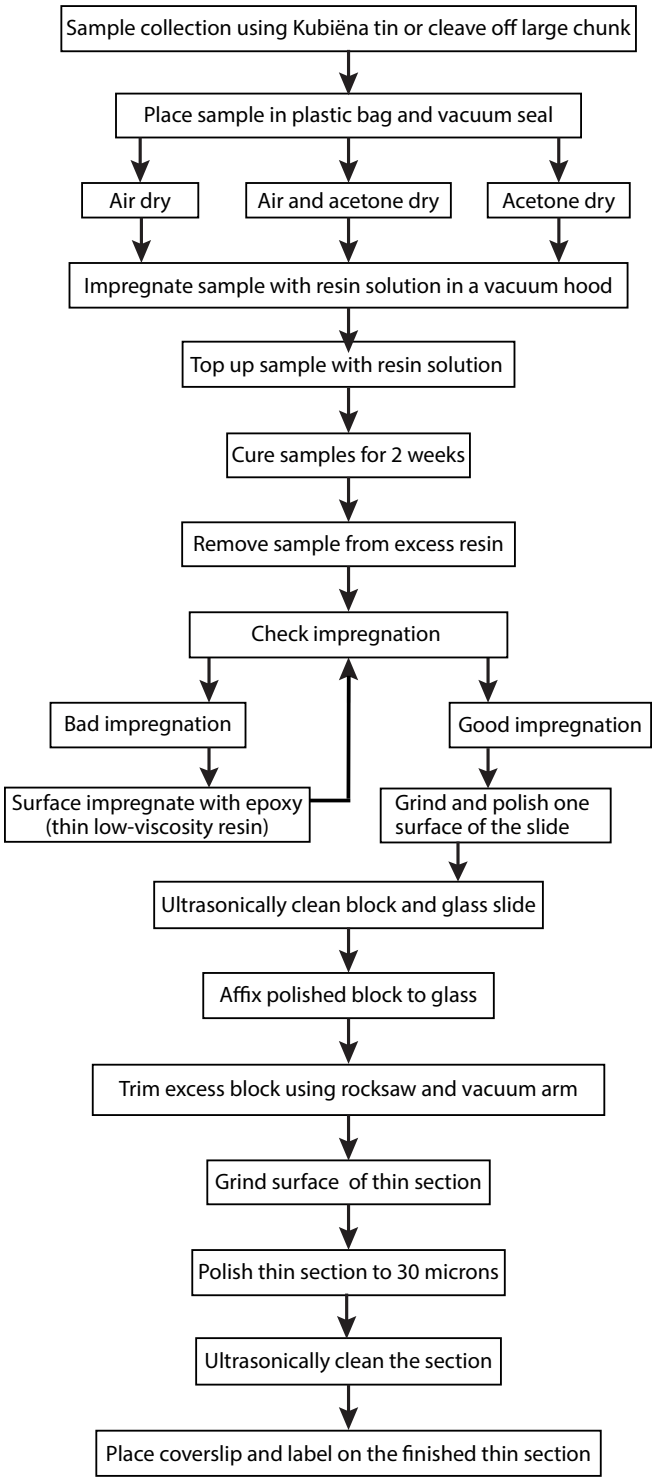

Figure 8. Flow chart desribing the medthology used in thin section production

structures (Fig. 9). As structures were identified, they were annotated on the high-resolution printed image of the thin section.

Once this initial microscopic analysis was completed, thin sections were placed on a PetroScope® projection macroscope under plain light (2X) and re-analyzed for confirmation of structures and to aid in the identification of any larger structures not recognized in thin section or through microscopic analysis. Although there is an admitted amount of personal bias in microstructure identification, a study conducted by Leighton et al. (2012) demonstrated that there is little difference in identification of structures due to human bias.

After the microstructures were identified and hand-annotated on the printed images, they were digitally added to the stitched image using Adobe Illustrator© CS6. Structures were annotated according to the legend (Appendix A) and placed over a semi-transparent copy of the original image. Several slides contained perfectly spherical dark air bubbles, which were either the result of the resin impregnation process, likely during the application of the cover slip, or the result of an air bubble being caught in the resin. It should also be noted that the arrows used to a indicate rotation structure *do not* reflect the direction of rotation, but are used to indicate the rotation of the material in general. The resulting annotated microstructures are not an exhaustive inventory of microstructures in the diamict, but rather a representation of major structures observed throughout the thin section and has been chosen to emphasize key structures and minimize cluttered labels on the annotated image.

Annotated slides were interpreted based on the specific microstructures within the thin section and their relationship to one another. Through this examination, a better understanding of the rheological conditions and the deformation of the diamict units can be inferred (Menzies et al., 1997; Carr, 1999; Carr et al., 2000; O'Cofaigh et al., 2005; Roberts and Hart, 2005). By looking at the sedimentological relationships (e.g. overprinting, deformation of structures, abundance) the cycle of deformation can also be determined (Menzies et al., 2010).

RESULTS

Sample intervals and stratigraphic units are shown in Figure 10. Complete field observations and sedimentological descriptions of each sampled unit (e.g. Unit A, Unit B, etc.) are described in Rice et al. (2013). Detailed micromorphological annotations are presented for each sample in Appendix A.

Unit A

Sample 11-PTA-022

There are two distinct domains: a darker, more clay-rich matrix (Appendix A, highlighted in yellow) and a lighter more clast-rich matrix, the latter of which comprises the majority of the thin section. There are small vug-like voids within this thin section. Two dominant lineation directions were observed: one in an upward northeast direction and a second trending down to the

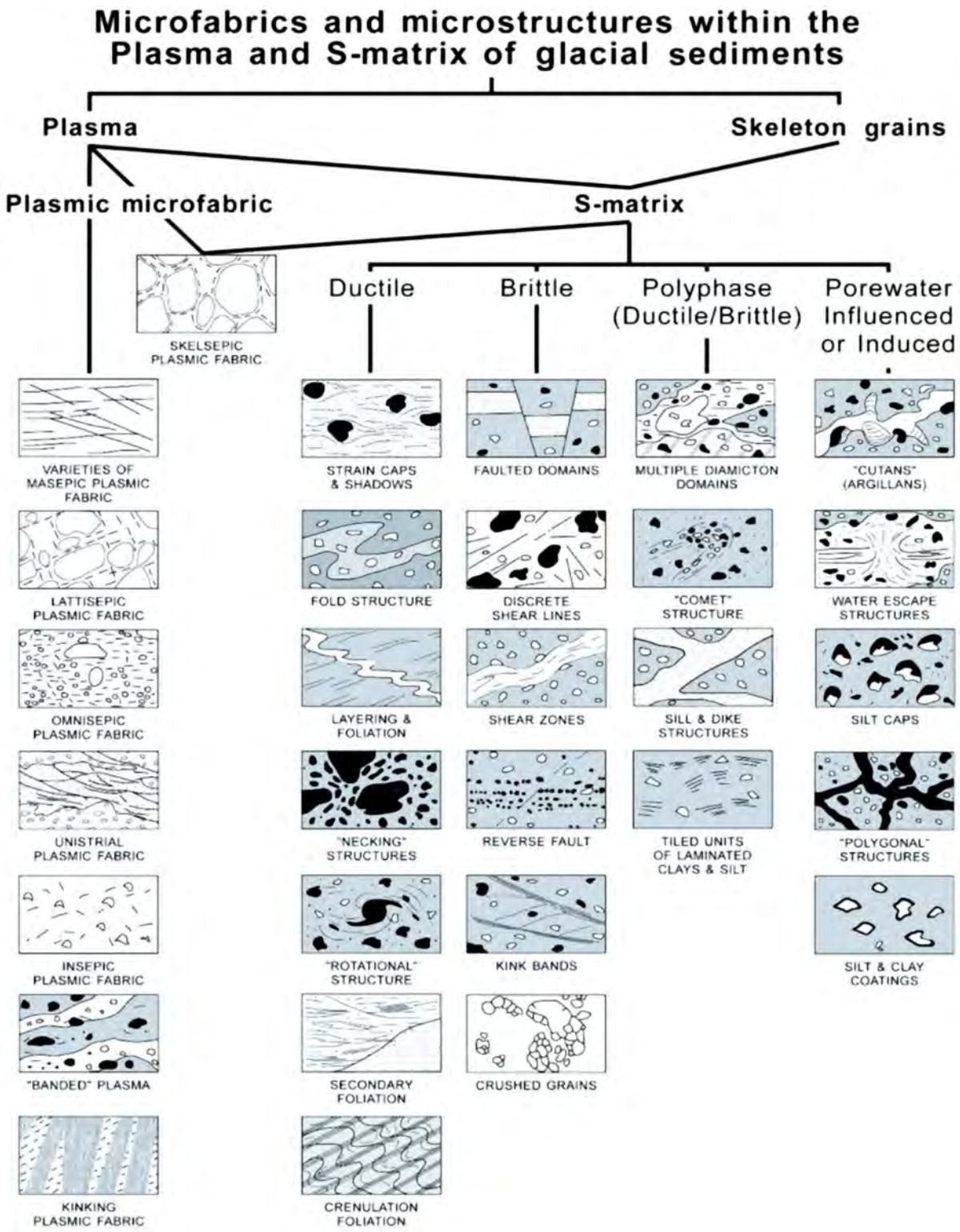

Figure 9. Chart showing the range of microstructures within the plasma and S-matrix of glacial sediments, listed under the primary influence of their creation (Table 3 of Menzies et al., 2006).

northeast. Some of the lineations display deformation curving. Grain-lineation sets parallel these lineations. An abundance of rotation structures have formed and transect the voids, indicating that the voids developed during the thin-section production.

Sample 11-PTA-023B

This sample consists mostly of a single matrix domain with a minor secondary matrix of darker composition (Appendix A, highlighted in yellow) observed around voids or clasts. Numerous fracture voids lie predomi-

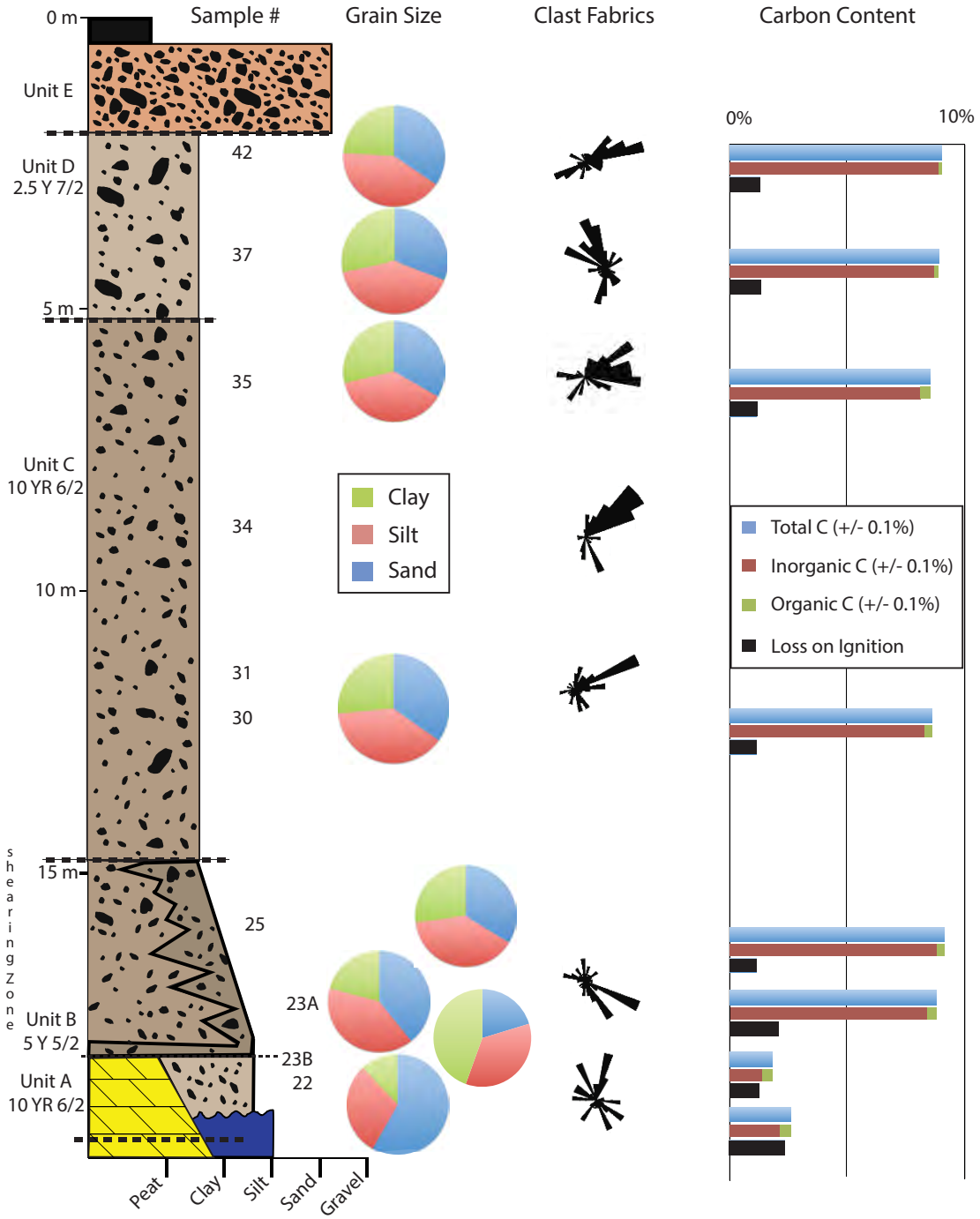

Figure 10. Stratigraphy and lithofacies of the northern exposure at open pit K-62. Bedrock is depicted to include the karst collapse structures that were seen in the open pits at Pine Point (Rice et al., 2013).

nantly in the horizontal and vertical planes. Lineations are seen throughout the sample but a higher concentration of lineations is found in the central portion of the slide. Rotation structures and grain-lineations parallel the fracture voids and general trend of the lineations.

Sample 11-PTA-023

This sample was collected at the contact between Unit A and the overlying Unit B. Unit A has a silt-rich matrix (36.95% sand and 40.39% silt); Unit B has a silty-sand matrix (58.17% sand and 29.86% silt). The difference in grain size is reflected in the till density; matrix from Unit A has been ripped up and reworked into the overlying Unit B. Rotation of the matrix can be seen in both Unit A and Unit B (Fig. 11).

Unit B

Sample 11-PTA-023A

Two distinct matrix domains are observed: a dark, clay-rich matrix and a light coarser matrix (Appendix A,

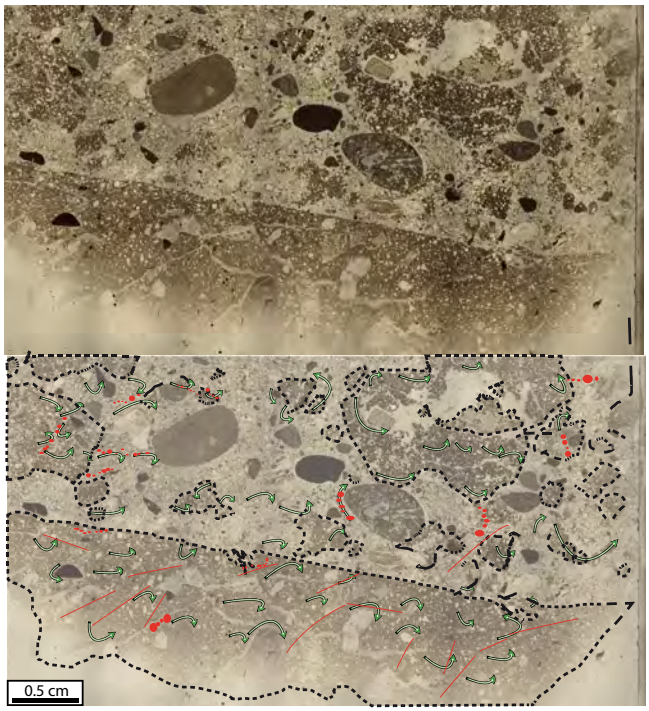

Figure 11. The top photograph is a thin section of sample 11-PTA-023. The bottom photograph is the same slide but has been annotated to highlight the contact between Unit A and Unit B. See legend in Appendix A for the description of annotations.

highlighted in yellow). Abundant rotation structures are found throughout the thin section. Several horizontal lineations and several grain stacks are perpendicular to these lineations, a number of which appear to be deformed. Microfractured grains and garmented grains are more abundant in the dark clay-rich matrix. This thin section contains few voids.

Unit C

Sample 11-PTA-025

Two distinct matrix domains are observed throughout Unit C: a dark clay-rich matrix and a light coarser matrix (Appendix A, highlighted in yellow). There is an abundance of void spaces, with some surrounding the larger clasts. Horizontal and vertical lineations are common, and a flow nose of densely packed grains was observed (Appendix A, outlined in by purple lines). There are several rotation structures, which appear predominantly toward the top of the section, likely due to the highly voidal matrix at the base of the section; this makes identification of structures in the thin section difficult. Zones of clay-dominant matrix composed of predominantly fine-grained material are also noted (Appendix A, highlighted in yellow). The inclusion of a foreign object in the slide likely occurred during the thin section production (Appendix A, highlighted in green).

Sample 11-PTA-026

This thin section contains a number of thin fracture voids, which have no defined orientation, and larger vug-like voids surrounding some larger grains. A thin shear zone (Appendix A, highlighted in red) separates two matrix types and may be associated with the fracture void located directly beneath it. There is an abundance of rotation structures, particularly bordering the two till domains. Lineations are oriented in two main directions: to the upper south corner of the slide and the lower south corner. Grain-lineations are parallel to these trends. Minor zones of clay accumulation are observed throughout the thin section.

Sample 11-PTA-027

A zone of deformational banding to the right of the largest clast in the thin section (Appendix A, highlighted in red) separates areas with darker and lighter matrices. The thin section contains a few fracture voids that angle to the top south corner of the slide and bottom south corner. A few lineations and grain-lineations are parallel to these voids, and rotation structures are observed around core clasts.

Sample 11-PTA-028

A zone of shear banding occurs in the upper north corner of this thin section. Several thin fracture voids are clustered on the north side. Lineations appear to be more abundant in the finer grained, darker domain and are predominantly oriented horizontally, as well as to the top north and bottom north sides. Grain-lineations are parallel to these orientations; some have been rotated. Rotation structures are abundant throughout the thin section. Microfractured grains appear along a fracture void edge (Appendix A, marked with an X), other fractured grains appear only in the darker, finer grained matrix.

Sample 11-PTA-029

This thin section contains large, vug-like voids in the sediment; thin fracture voids with no predominant direction have also been noted. Lineations are oriented from the bottom north corner to the top south corner. The angle of these lineations decreases toward the south, near the base of the thin section. Grain stacks are generally oriented perpendicular to the surrounding lineations. Rotation, galaxy, necking structures, and pressure shadows on the north side of some clasts are all observed in both domains.

Sample 11-PTA-030

A single domain with a small darker zone is preserved in this thin section (Appendix A, highlighted in yellow). This may represent bitumen from the bedrock in the region (cf. Rhodes et al., 1984; Lemmen, 1990;

Gleeson and Turner, 2007; Oviatt, 2013) or an accumulation of clay. Most voids observed in this thin section have no clear orientations. Lineations are oriented in two directions: from the top north-northwest to bottom south-southeast and from the bottom north-northwest to top south-southeast. Grain-lineation orientations are parallel to the direction of the lineations and rotation structures and appear mainly around medium-size granules. There is evidence of pipe-like pore-water flow (Appendix A, highlighted in blue) through the slide (orthogonal to the plane of the slide). Minor grain crushing is observed throughout the slide. The lower portion of the sample exhibits a large concentration of small voids indicative of brecciation.

Sample 11-PTA-031

Lineations are oriented predominantly to the top southeast, crosscutting to the lower southeast. Grain stacks and stacked rotation structures are parallel to the lineation and grain-lineation orientations. Rotation structures are more abundant in the lighter, coarser grained matrix. Rotation structures have not formed near lineations. Pressure shadows are observed adjacent to some larger clasts. There is a weak orientation of what appears to be the a-axis (long axis) of small clasts to the top southeast corner of the slide.

Sample 11-PTA-032

A number of lineations are oriented to the top northeast corner and bottom northeast corners of the slide. Grain-lineations are parallel to these lineations and are angled toward the top northeast corner. Rotation structures are weakly parallel to the orientations of the grain-lineations and lineations. Minor pressure shadows occur in the lighter, coarser matrix. A necking structure was also identified.

Sample 11-PTA-035

This sample was packed in fine sand for shipping, which can be seen along the outer edges of the sample (Appendix A, highlighted in white). A number of lineations are oriented to the top northeast and lower northeast corners of the slide. Fine-grained grain-stacks occur parallel to the orientation of these lineations, i.e., toward the upper northeast corner, although some stacks have been rotated. Rotation structures have no clearly preferred stacking orientation. The apparent a-axis of some elongated grains displays a weak orientation to the top northeast corner.

Sample 11-PTA-036

This thin section contains lineations oriented predominantly to the top northeast corner of the slide. Although, there are also some lineations oriented in the lower northeast direction. Grain-lineations are parallel to the lineations oriented to the lower northeast corner of the slide. Weakly developed rotation structures are also observed. Grain crushing has occurred throughout the matrix.

Unit D

Sample 11-PTA-037

There are two large fracture voids: one oriented vertically through the thin section, and the other oriented towards the top southwest. An additional large void on the northeast side developed during the production of the thin section. A number of lineations are visible throughout the thin section, predominantly orientated to the bottom northeast and top northeast corners of the slide. Grain-lineations align parallel to the top northeast lineations. Rotation structures, several ‘groups’ of which aligned towards the top northeast corner, are parallel to the second set of lineations and most grain stacks. Pressure shadows and clay accumulations are also visible in the southwest (bottom) side of some larger clasts.

Sample 11-PTA-038

This sample was packed in fine sand for shipping, which can be seen surrounding the sample (Appendix A, highlighted in white). Two matrix textures have been observed in the thin section: a darker clay-rich domain and a lighter coarser domain (Appendix A, highlighted in yellow). Abundant crosscutting lineations are present, oriented toward the top northeast and lower northeast corners of the slide. Several horizontal fracture voids are noted near the base of the slide. Grain-lineations in the matrix trend horizontally; rotation structures align in a more vertical trend.

Sample 11-PTA-040

There are a large number of voids oriented in all directions throughout this thin section. Short lineations have a slightly preferred horizontal orientation; and there are a few parallel grain-lineations. Rotational structures have no clear orientation. A few crushed grains have been identified throughout the thin section.

Sample 11-PTA-041

This slide contains a large number of voids that have a preferred vertical orientation. Several short lineations are oriented toward the lower east-southeast bottom corner. Grain-lineations occur near the base of the slide and are parallel to the short lineations. Rotation structures and microfractured grains are most abundant in the upper portion of the thin section.

Sample 11-PTA-042

A plethora of voids are observed in the thin section. Several large grains are well rounded and have an ori-

entation similar to the voids. However, this sample was collected too proximal to the land surface to be able to conclude that all its structures were glacially influenced. The large voids in the thin section can likely be attributed to natural soil processes and exposure to anthropologic activity at the former open pit. Annotations have not been added to this image.

DISCUSSION

Specific microstructures that have been identified (cf. van der Meer, 1993; Menzies, 2000; van der Meer and Menzies, 2006; Menzies et al., 2012) and observations made by Rice et al. (2013) confirm that the samples collected from pit K-62 are of glacial origin (i.e. till). In addition, the presence of multiple domains, rip-up microstructures (Fig. 11), multi-directional lineations, rotation structures, and deformed grain lineations indicate that the till was emplaced by a mobile bed being eroded and incorporated into underlying immobile till units.

Unit A

The two domains sampled in Unit A could be separate domains that have not completely homogenized, or they could be indicative of a zone of high shearing. The absence of grains suggests that this was likely the reworked sand lens that has been previously reported in this unit (see Rice et al., 2013). Voids in the thin section appear to be the result of thin section production. However, some of the more linear voids in the upper sample (11-PTA-023B) exemplify the fissility of the till and the plane of shear within it (van der Meer 1996, 1997; Carr, 2004). The abundance of lineations indicates the sediment has undergone a high degree of shearing. The preferred orientation of grain stacks in two directions indicates some overprinting has accompanied the stress changes experienced by the diamicton; these ductile structures tend to form at an oblique angle to the shearing direction (Hatcher, 1990). The abundance of rotation structures illustrates the ductile deformation of the sediment. The abundance of rotation structures within the upper portion of the unit in conjunction with the lack of fissility in the lower section, suggests that the overlying glacial stress did not penetrate through the entire unit, either due to fluctuating shear stress during deposition or pore-water fluctuation. There is no evidence of pore-water escape structures, indicating that there was a flux in the shear stress. Rafting of material in this unit (Fig. 11) implies that this till unit was ripped up, introducing rafted older sediments into the mobile deforming subglacial bed. The scarcity and small size of these inclusions makes it difficult to postulate a sediment type. However, the constraint of these inclusions to clasts and void spaces, possibly of removed clasts, indicates the reworked sediment likely was very cohesive. None of the clasts associated with these inclusions appear to be derived from the local bedrock, which indicates considerable transportation distance.

Unit B

Only one sample was collected from Unit B (sample 11-PTA-023A) as this unit was not thick enough to justify additional samples. Multiple domains within the thin section demonstrate how Unit A was reworked into Unit B, but not completely homogenized. Rotation structures are indicators of matrix deformation as the two till units mixed. Relatively long lineations suggest a significant amount of overriding shear stress transcended both domains, indicating that the overriding stress occurred after the majority of mixing and deformation occurred. There is also a clear shift in glacial dynamics in the overlying unit (Unit C), as sediment was reworked and incorporated into the underlying unit (Unit B), which can be observed at the contact between these two units (sample 11-PTA-023, Fig. 11).

Unit C

Unit C is the thickest unit described in the section (~10 m), and was the most abundantly sampled. In total, twelve micromorphological samples were collected from the unit; six of which (samples 11-PTA-025 to -030) were sampled along the lower shearing contact with unit B. These six samples (Fig. 10) have very similar structures, exhibiting only slight changes. Multiple domains are contained in each of these six samples, indicating Unit B was re-worked into Unit C but was not fully homogenized. Lineations observed in thin section transcend both domains, indicating that the external stress that created these lineations occurred post-mixing of the two units. Rotation structures throughout this unit are more abundant in the clay-rich domains. These clay-rich domains may have had higher pore water content, allowing the movement and rotations of fine grains with less resistance.

The vug-like voids in the thin sections likely formed during the production of the slides as fracture voids can be a result of the drying process. However, it cannot be ruled out that these voids are not in situ. Grains edging these voids do not parallel the voids, indicating that the voids were not induced by shear during post-depositional unloading or during ice-lens formation (van Vliet-Lanoë et al., 1984; Sveistrup et al., 2005). Drying fractures do extenuate pre-existing zones of weakness associated with the fissility of the till and are therefor the likely causation.

Zones of shear banding (Appendix A, sample 11-PTA-027, highlighted in red) indicate an increase in shear stress associated with changing subglacial conditions in transitional zones, which could include basal

ice strain, the rheology of subjacent deforming sediment, and/or temperature (Truffer et al., 2000; van der Meer et al., 2003; Larsen et al., 2007; Phillips et al., 2008; Boulton, 2010). The upper-most sample collected from this shearing zone (sample 11-PTA-030) contains a water escape structure overlying a moderately brecciated matrix. This structure indicates pore water was released near the upper portion of the thin section, with pipe-like groundwater flow toward either the east or west (into or out of the image). As a result of the pore water draining from the matrix, strain on the underlying sediment increased, causing an influx in shear and possibly brecciating the matrix.

Samples 11-PTA-031 and 11-PTA-032, which were collected just above this shear contact, contain two separate domains, indicating that the mixing of the two units was continual even away from the shear contact.

Lineations have two predominant directions that crosscut both domains, suggesting mixing occurred prior to the formation of the lineations. Grain stacks throughout the thin section are parallel to the predominant lineation orientations. The large number of lineations and grain stacks in these samples is a possible indication of increasing basal shear stress. There is also an abundance of rotation structures, which are constrained in separate domains. The abundance of crushed grains in the lighter matrix may also indicate that the mixing occurred under higher strain.

The remaining samples from Unit C were collected above this shear contact, within 2 m of the upper contact with Unit D. Both samples were very fissile and only small chunks cleaved from the face could be collected. The lower of the two samples (11-PTA-035) shows multiple domains, which indicates continual mixing occurred throughout the unit. Rotation structures, the lack of edge-to-edge crushing, and a single predominant lineation direction all suggest that this *may* have been deposited by fast-flowing ice (cf. Menzies et al., 2012). Sample 11-PTA-036 has an abundance of crushed grains and lineations, indicative of shearing. However, the abundance of rotation structures and curved lineations implies this was likely a polyphase deformation event.

Unit D

The remaining five samples were collected from Unit D. All thin sections from this unit display very similar structures. The lower two samples (11-PTA-037 and -38) contain abundant lineations that have a single general direction in the upper sample but exhibit some crosscutting in the lower sample. Rotation structures indicate that deformation occurred throughout the unit. Stream-lined landforms in the area (Rice et al., 2013) and a lack of grain fracturing within this unit are suggestive of ice streaming (Menzies, et al., 2012), although the highly fragmented matrix and limited number of samples collected makes this conclusion difficult to confirm. The two overlying samples (11-PTA-040 and -041) show highly fractured matrices that contain microstructures unrelated to their orientation and distribution. These voids were likely produced by repeated cycles of freeze and thaw (seasonal frost). The highly fractured matrices are too disturbed for accurate micromorphological interpretation (Pawluk, 1988).The upper-most sample (11-PTA-042) was collected very close to the ground surface and thus soil-forming processes and horizonation may have been destroyed by the anthropogenic influence of heavy mining equipment.

CONCLUSION

This study has demonstrated that micromorphology can be a useful tool in augmenting information gained from field observations, and provide additional sedimentological support to interpretations of stratigraphy and depositional environment. However, one must remember that the samples examined in this paper are only a small portion of the entire sedimentary sequence and that micromorphology is a tool that should be used in conjunction with other sedimentological tools to study glacial sediments and understand past glacial dynamics.

In this study, micromorphological samples and their interpretations support field observation of four distinct till units at the Pine Point mine site (Rice et al., 2013). Each till unit appears to have been deposited in a subglacial environment by active layer mixing and deformation over an underlying immobile unit.

ACKNOWLEDGEMENTS

This research was funded by the GSC's Geo-Mapping for Energy and Minerals (GEM) Program (2008-2013) under the Tri-Territorial Indicator Mineral Project. The authors would like to thank Natasha Oviatt (University of Alberta) for her enthusiastic assistance in the field and Martin Ouellette (Brock University) for his meticulous work in the production of the thin sections. A special thanks to David Huntley (GSC-Vancouver) for his critical review and edits on this work.

REFERENCES

Baroni, C. and Fasano, F., 2006. Micromorphological evidence of warm-based glacier deposition from the Ricker Hills Tillite (Victoria Land, Antarctica); Quaternary Science Reviews, v. 25, p. 976–992.

Bostock, H.S., 1970. Physiographic regions of Canada; Geological Survey of Canada, Map 1254A, scale 1:5,000,000.

Boulton, G.S., 1976. The origin of glacially-fluted surfaces- observations and theory; Journal of Glaciology, v. 17, p. 287–309.

Boulton, G., 2010. Drainage pathways beneath ice sheets and their implications for ice sheet form and flow: the example of the British Ice Sheet during the last glacial maximum; Journal of

Quaternary Science, v. 25, p. 483–500.

Carr, S.J., 1999. The micromorphology of Last Glacial Maximum sediments in the Southern North Sea; Catena, v. 35, p. 123–145.

Carr, S.J., 2001. Micromorphological criteria for discriminating subglacial and glacimarine sediments: evidence from a contemporary tidewater glacier, Spitsbergen; Quaternary International, v. 86, p. 71–79.

Carr, S.J., 2004. Micro-scale features and Structures, Chapter 6 *In:* A Practical Guide to the Study of Glacial Sediments, (ed.) D.J.A. Evans and D.I. Benn; Hodder, London, UK, p. 115–144.

Carr, S.J. and Lee, J.R., 1998. Thin section production of diamicts: Problems, and solutions; Journal of Sedimentary Research, v. 68, p. 217–220.

Carr, S.J., Haflidason, H., and Sejrup, H.P., 2000. Micromorphological evidence supporting late Weichselian glaciation of the northern North Sea; Boreas, v. 29, p. 315-328.

Dreimanis, A., 1982. INQUA — Commission on genesis and lithology of Quaternary deposits. Work Group (1) — Genetic classification of tills and criteria for their differentiation. Progress report on activities 1977–1982, and definitions of glaciogenic terms, *In:* INQUA Commission on Genesis and Lithology of Quaternary Deposits, Report on Activities 1977–1982, (ed.) C. Schluchter; Zurich, p. 12–31.

Fitzpatrick, E.A., 1984. Micromorphology of Soils; London, Chapman and Hall, 433 p.

Gleeson, S.A. and Turner, W.A., 2007. Fluid inclusion constraints on the origin of the brines responsible for Pb-Zn mineralization at Pine Point and coarse non-saddle and saddle dolomite formation in southern Northwest Territories. Geofluids, no. 7, p. 51–86.

Hannigan, P., 2007. Metallogeny of the Pine Point Mississippi Valley-type lead-zinc district, southern Northwest Territories, *In:* Mineral Deposits of Canada: A Synthesis of Major Deposit Types, District Metallogeny, the Evolution of Geological Provinces, and Exploration Methods, (ed.) W.D. Goodfellow; Geological Association of Canada, Mineral Deposits Division, Special Publication no. 5, p. 609–632.

Hatcher, R.D., Jr., 1990. Structural Geology, Principles, Concepts, and Problems; Macmillan, New York, New York, 531 p.

Hiemstra, J.F. and Rijsdijk, K.F., 2003. Observing artificially induced strain: implications for subglacial deformation; Journal of Quaternary Science, v. 18, p. 373–383.

Kemp, R.A., 1985. Soil micromorphology and the Quaternary; Quaternary Research Association, Technical guide no. 2, p. 80.

Larsen, N.K., Piotrowski, J.A., and Menzies, J., 2007. Microstructural evidence of low-strain, time transgressive subglacial deformation; Journal of Quaternary Science, v. 22, p. 593–608.

Lee, J. and Kemp, R., 1993. Thin sections of unconsolidated sediments and soils: a recipe; Center for Environmental Analysis and management (CEAM), Royal Holloway, University of London, Technical Report, v. 2, p. 1–32.

Leighton, I.D., Hiemstra, J.F., and Weidemann, C.T., 2012. Recognition of micro-scale deformation structures in glacial sediments- pattern perception, observer bias and the influence of experience; Boreas, v. 42, p. 463–469.

Lemmen, D.S., 1990. Surficial materials associated with glacial Lake McConnell, southern District of Mackenzie, *In:* Current Research, Part D; Geological Survey of Canada, Paper 90-1D, p. 79–83.

Lemmen, D.S., 1998a. Surficial geology, Klewi River, District of Mackenzie, Northwest Territories; Geological Survey of Canada, Map 1905A, scale 1:250 000. doi:10.4095/209686

Lemmen, D.S., 1998b. Surficial geology, Buffalo Lake, District of Mackenzie, Northwest Territories; Geological Survey of Canada, Map 1906A, scale 1:250 000. doi:10.4095/209687

Lemmen, D.S., Duk-Rodkin, A., and Bednarski, J.M., 1994. Late glacial drainage systems along the northwestern margin of the Laurentide Ice Sheet; Quaternary Science Reviews, v.13, p. 805–828.

McClenaghan, M.B., Oviatt, N.M., Averill, S.A., Paulen, R.C., Gleeson, S.A., McNeil, R.J., McCurdy, M.W., Paradis, S., and Rice, J.M., 2012. Indicator mineral abundance data for bedrock, till and stream sediment samples from the Pine Point Mississippi Valley-type Zn-Pb deposits, Northwest Territories; Geological Survey of Canada, Open File 7267. doi:10.4095/292121

Menzies, J., 2000. Micromorphological analysis of microfabrics and microstructures indicative of deformational processes in glacial sediments, In Deformation of Glacial Materials, (ed.) A.J. Maltman, B. Hubbard, and M.J. Hambrey; Geological Society Special Publication 176, London, p. 245–258.

Menzies, J. and Maltman, A.J., 1992. Microstructures in diamictons – evidence of subglacial bed conditions; Geomorphology, v. 6, p. 27–40.

Menzies, J., Zaniewski, K., and Dreger, D., 1997. Evidence, from microstructures, of deformable bed conditions within drumlins, Chimney Bluffs, New York State; Sedimentary Geology, v. 111, p. 161–175.

Menzies, J., van der Meer, J.J.M., and Rose, J., 2006. Till – as a glacial "tectomict", its internal architecture, and the development of a "typing" method for till differentiation; Geomorphology, v. 75, p. 172–200.

Menzies, J., van der Meer, J.J.M., Domack, E., and Wellner, J.S., 2010. Micromorphology: As a tool in the detection analyses and interpretation of glacial sediments and man-made materials; Proceedings of the Geologists' Association, v. 121, p. 281–292.

Menzies, J., Gao, C., and Kodors, C., 2012. Micromorphology of a Middle Pliocene till from the James Bay Lowlands, Canada, evidence of fast ice stream or surge behaviour; Proceedings of the Geologists' Association, v. 124, p. 790–801.

Murphy, C.P., 1986. Thin section preparation of soils and sediments; AB Academic, University of Michigan, 149 p.

O'Cofaigh, C., Dowdeswell, J.A., Allen, C.S., Hiemstra, J.F., Pudsey, C.J., Evens, J., and Evans, D.J.A., 2005. Flow dynamics and till genesis associated with a marine-based Antarctic paleo-ice stream; Quaternary Science Reviews, v. 24, p. 547–561.

Okulitch, A.V., 2006. Phanerozoic bedrock geology, Slave River, District of Mackenzie, Northwest Territories; Geological Survey of Canada, Open File 5281, scale 1:1 000 000. doi:10.4095/223451

Oviatt, N.M., 2013. Characterization of indicator minerals and till geochemical dispersal patterns associated with the Pine Point Pb-Zn Mississippi Valley-type deposits Northwest Territories, Canada; M.Sc. thesis, Earth and Atmospheric Sciences, University of Alberta, Edmonton.

Oviatt, N.M. and Paulen, R.C., 2013. Surficial geology, Breynat Point, Northwest Territories, NTS 85-B/15; Geological Survey of Canada, Canadian Geoscience Map 114, scale 1:50 000. doi:10.4095/292247

Oviatt, N., Paulen, R.C., McClenaghan, M.B., Gleeson, S.A., and Paradis, S., 2011. Drift prospecting research at the Pine Point Pb-Zn Mississippi Valley Type (MVT) deposit, Northwest Territories; Geohydro 2011, Québec, 1 p.

Paulen, R.C., Prior, G.J., Plouffe, A., Smith, I.R., McCurdy. M.W., and Friske, P.W.B., 2007. Cretaceous shale of northern Alberta: A new frontier for base metal exploration, *In:* Exploration in the New Millennium, (ed.) B. Milkereit; Proceedings of the Fifth Decennial International Conference on Mineral Exploration, p. 1207–1213.

Paulen, R.C., Paradis, S., Plouffe, A., and Smith, I.R., 2011. Pb and S isotopic composition of indicator minerals in glacial sediments from northwest Alberta, Canada: implications for Zn-Pb base metal exploration; Geochemistry Exploration Environment Analysis, v. 11, p. 309–320.

Pawluk, S., 1988. Freeze-thaw effects on granular structure reorganization for soil materials of varying texture and moisture content; Canadian Journal of Soil Sciences, v. 68, p. 485–494.

Phillips, E., Lee, J.R., and Burke, H., 2008. Progressive proglacial to subglacial deformation and syntectonic sedimentation at the margins of the Mid-Pleistocene British Ice Sheet: evidence from north Norfolk UK; Quaternary Science Reviews, v. 27, p. 1848–1871.

Prest, V.K., Grant, D.R., and Rampton, V.N., 1968. Glacial map of Canada; Geological Survey of Canada, Map 1253A, scale 1:5 000 000. doi:10.4095/108979

Rhodes, D., Lantos, E.A., Lantos, J.A., Webb, R.J., and Owens, D.C., 1984. Pine Point Orebodies and their relationship to the stratigraphy, structure, dolomitization, and karstification of the Middle Devonian Barrier Complex; Economic Geology, v. 79, p. 991–1055.

Rice, J.M., Paulen, R.C., Menzies, J., McClenaghan, M.B., and Oviatt, N.M., 2013. Glacial stratigraphy of the Pine Point Pb-Zn mine site, Northwest Territories; Geological Survey of Canada, Current Research 2013-5, p. 1–14. doi:10.4095/292184

Roberts, D.H. and Hart, J.K., 2005. The deforming bed characteristics of a stratified till assemblage in northeast Angila, UK: Investigating controls on sediment rheology and strain signatures; Quaternary Science Reviews, v. 24, p. 123–140.

Sveistrup, T.E., Haraldsen, T.K., Langohr, R., Marcelino, V., and Kværner, J., 2005. Impact of land use and seasonal freezing on morphological and physical properties of silty Norwegian soils; Soil and Tillage Research, v. 8, p. 39–56.

Truffer, M., Harrison, W.D., and Echelmeyer, K.A., 2000. Glacier motion dominated by processes deep in underlying till; Journal of Glaciology, v. 46, p. 213–221.

van der Meer, J.J.M., 1987. Micromorphology of glacial sediments as a tool in distinguishing genetic varieties of till; Geological Survey Finland, Special Paper 3, p. 77–89.

van der Meer, J.J.M., 1993. Microscopic evidence of subglacial deformation; Quaternary Science Reviews, v. 12, p. 553–587.

van der Meer, J.J.M., 1996. Micromorphology, *In:* Past Glacial Environments – Sediments, Forms and Techniques, vol. 2, (ed.) J. Menzies; Butterworth-Heinemann, Oxford, p. 335–356.

van der Meer, J.J.M., 1997. Particle and aggregate mobility in till: Microscopic evidence of subglacial processes; Quaternary Science Reviews, v. 16, p. 827–831.

van der Meer, J.J.M. and Menzies, J., 2006. Sixth International workshop on the micromorphology of glacial sediments; Department of Geosciences, Hamilton College, Clinton, New York, p. 1–83.

van der Meer, J.J.M., Menzies, J., and Rose, J., 2003. Subglacial till: the deforming glacier bed; Quaternary Science Reviews, v. 22, p. 1659–1685.

van Vliet-Lanoë, B., Coutard, J.P., and Pissart, A., 1984. Structures caused by repeated freezing and thawing in various loamy sediments: a comparison of active, fossil and experimental data; Earth Surface Processes and Landforms, v. 9, p. 553–565.

APPENDIX A. Annotated thin sections.

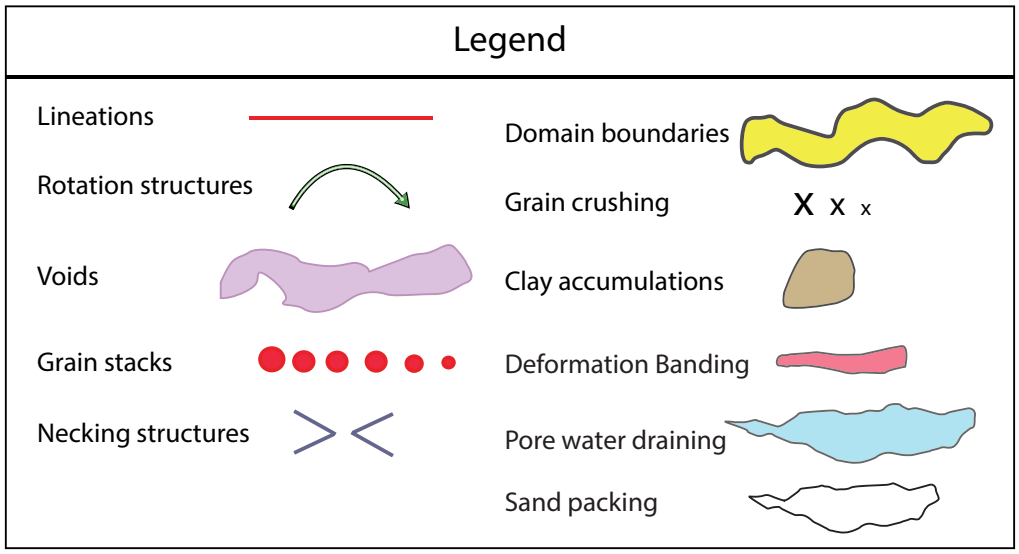

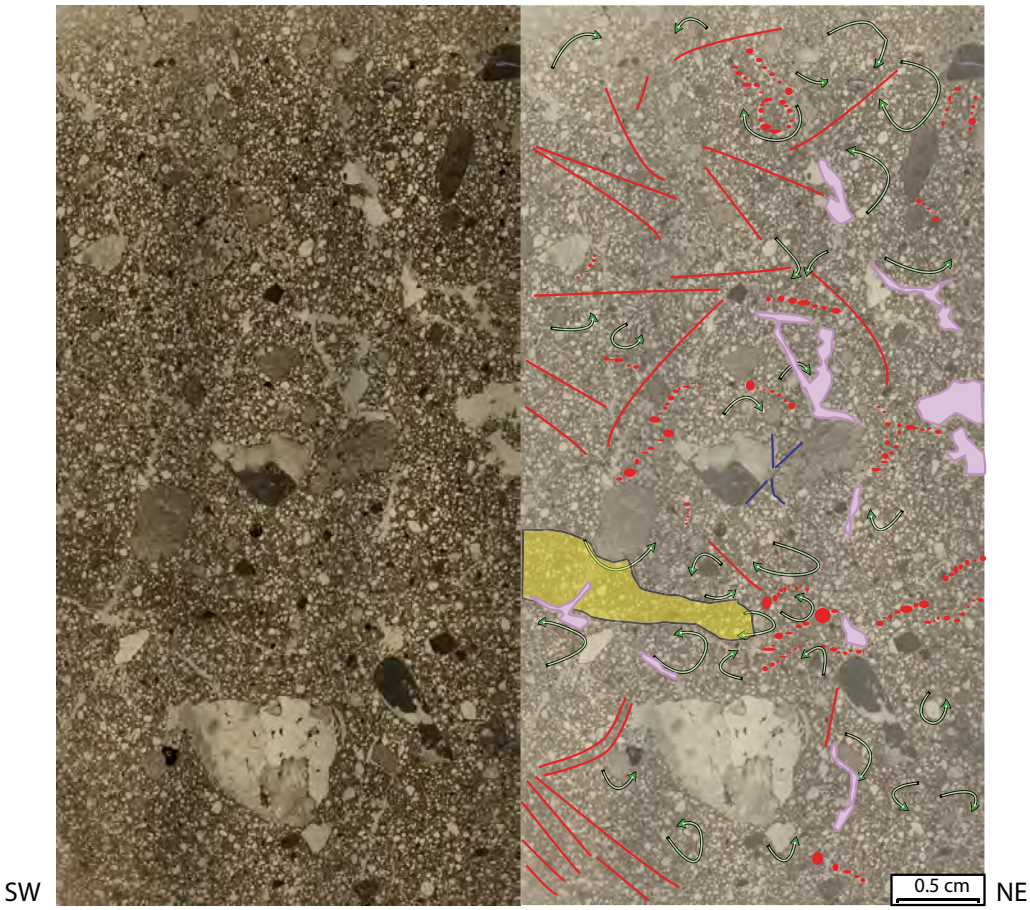

Sample 11-PTA-022. This sample was collected at an azimuth of 315°.

APPENDIX A continued.

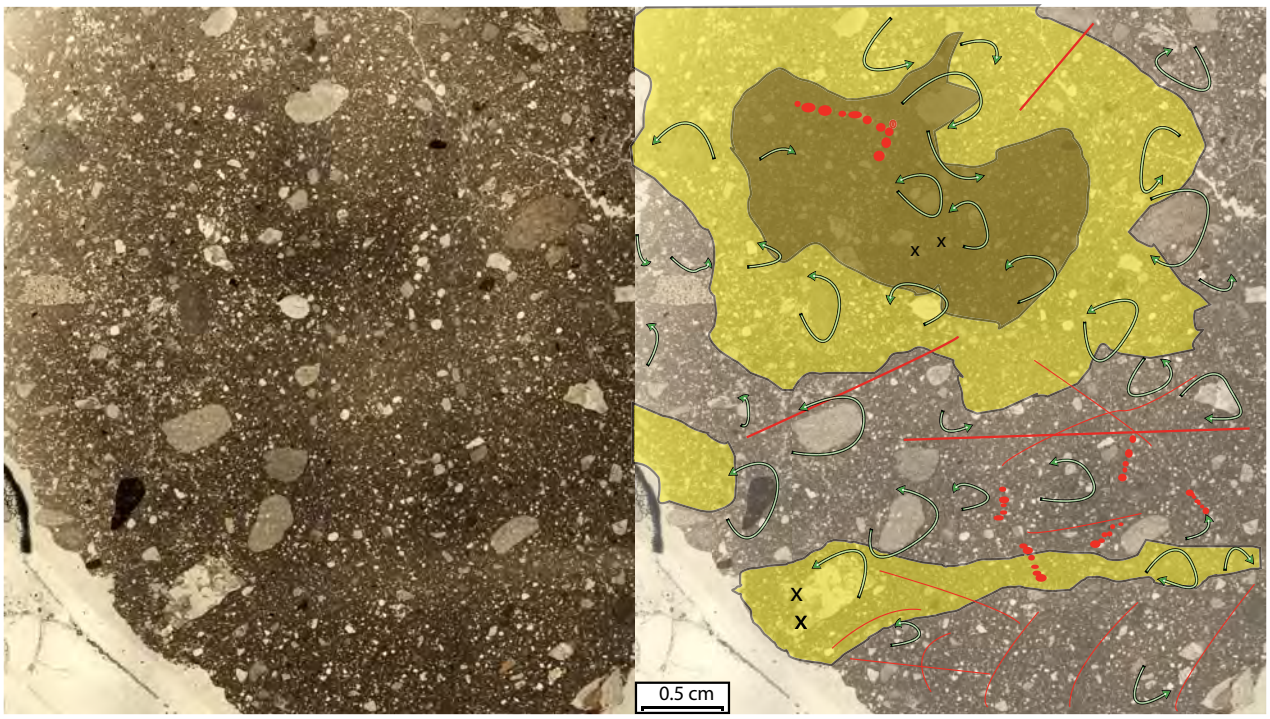

WSW ENE

Sample 11-PTA-023A. This sample was collected at an azimuth of 350°.

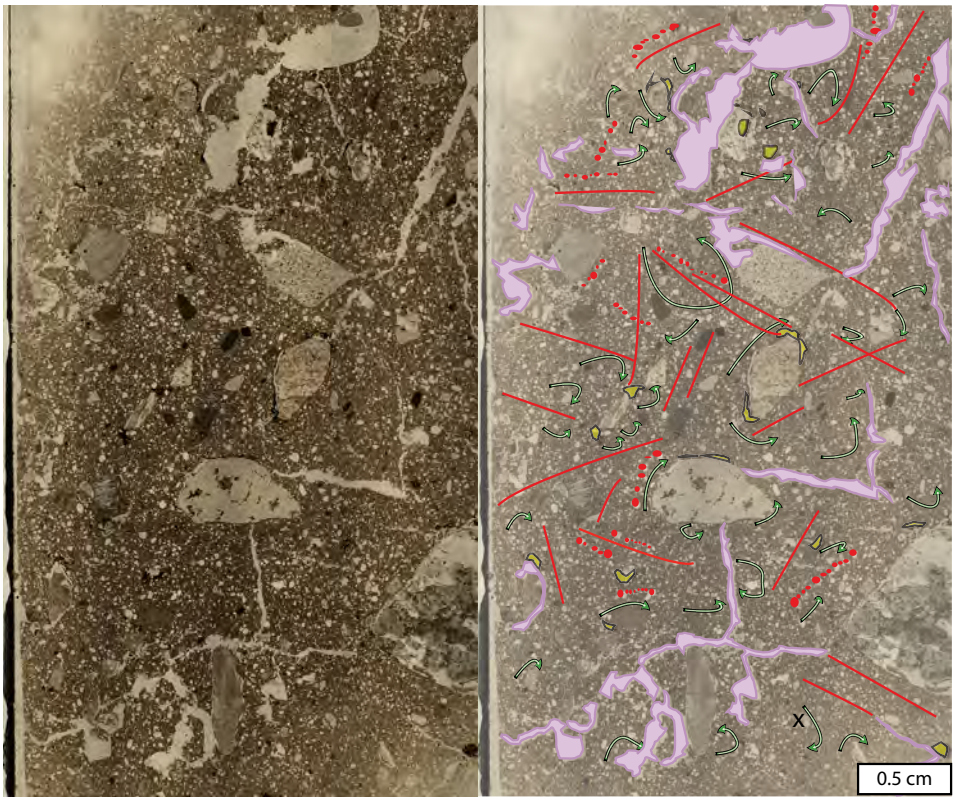

SWS ENE

Sample 11-PTA-023B. This sample was collected at an azimuth of 345°.

APPENDIX A continued.

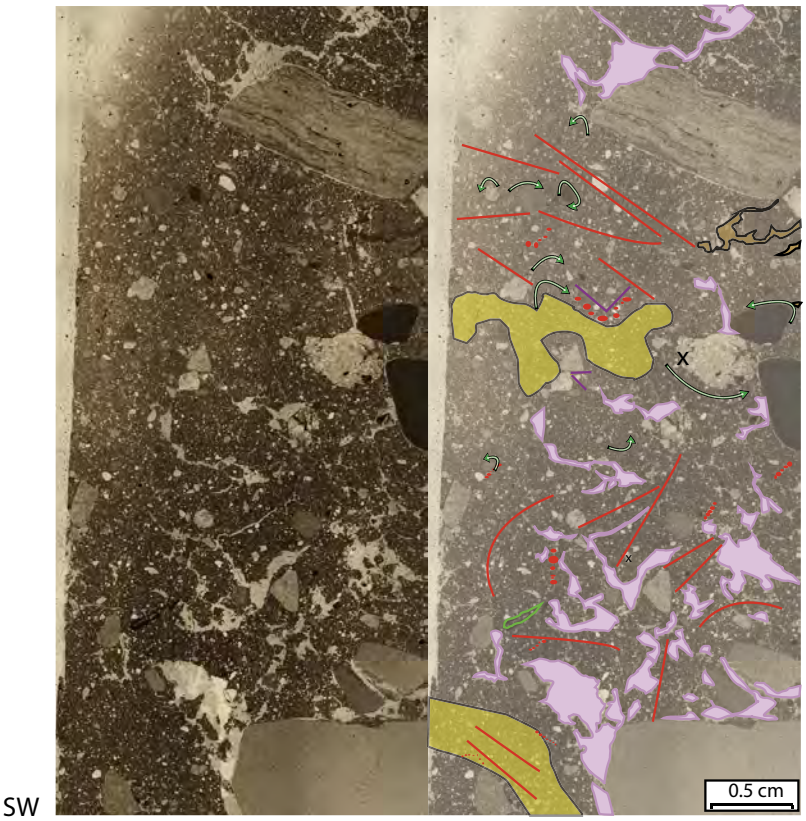

Sample 11-PTA-025. This sample was collected at an azimuth of 300°.

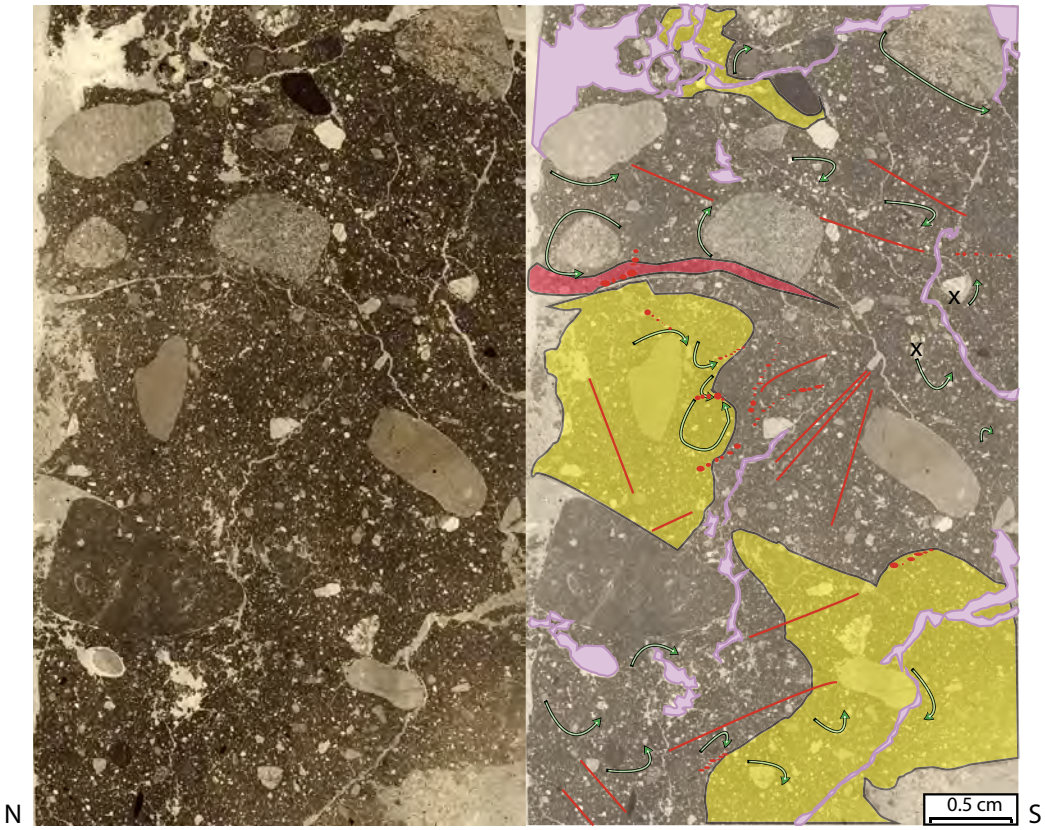

Sample 11-PTA-026. This sample was collected at an azimuth of 095°.

APPENDIX A continued.

Sample 11-PTA-027.
This sample was collected at an azimuth of 095°.

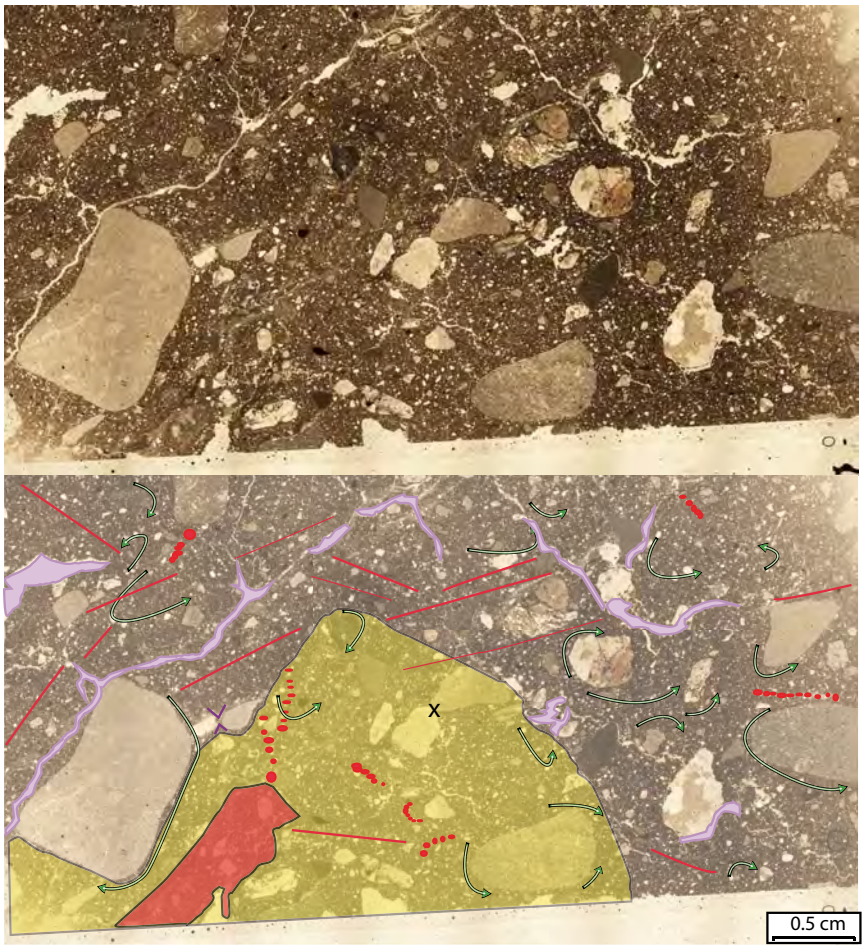

Sample 11-PTA-028.
This sample was collected at an azimuth of 095°.

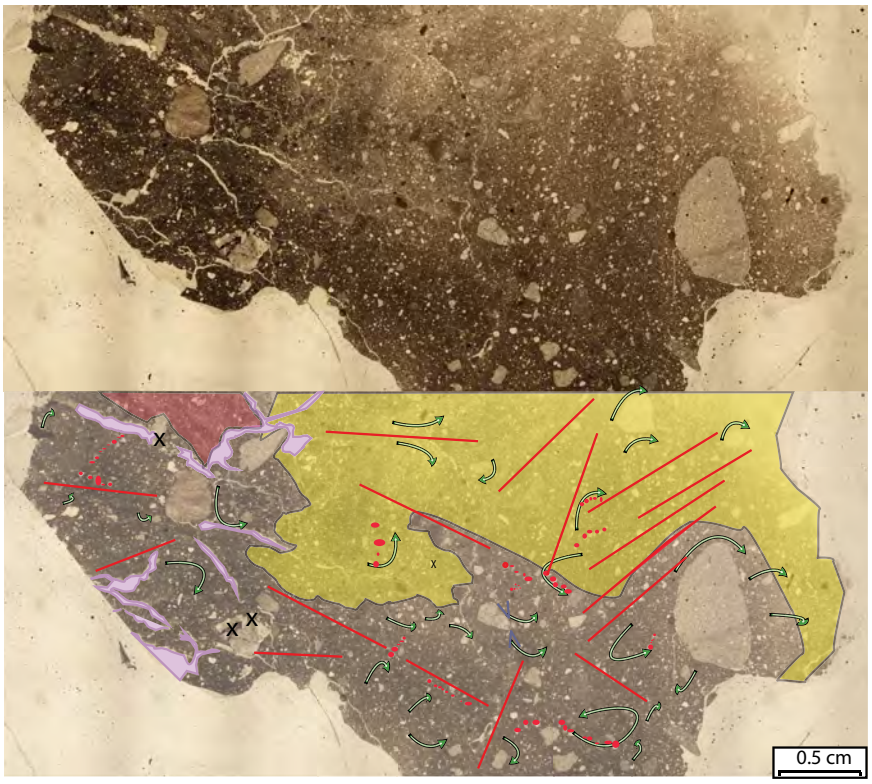

APPENDIX A continued.

Sample 11-PTA-029.
This sample was collected at an azimuth of 095°.

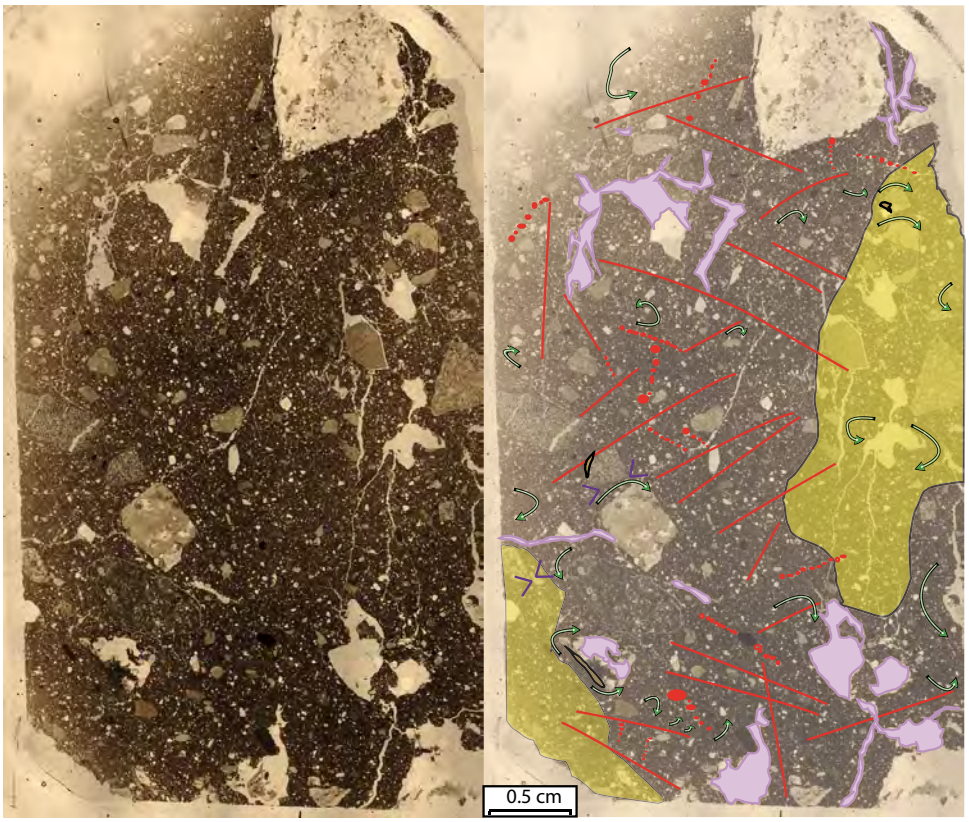

Sample 11-PTA-030.
This sample was collected at an azimuth of 062°.

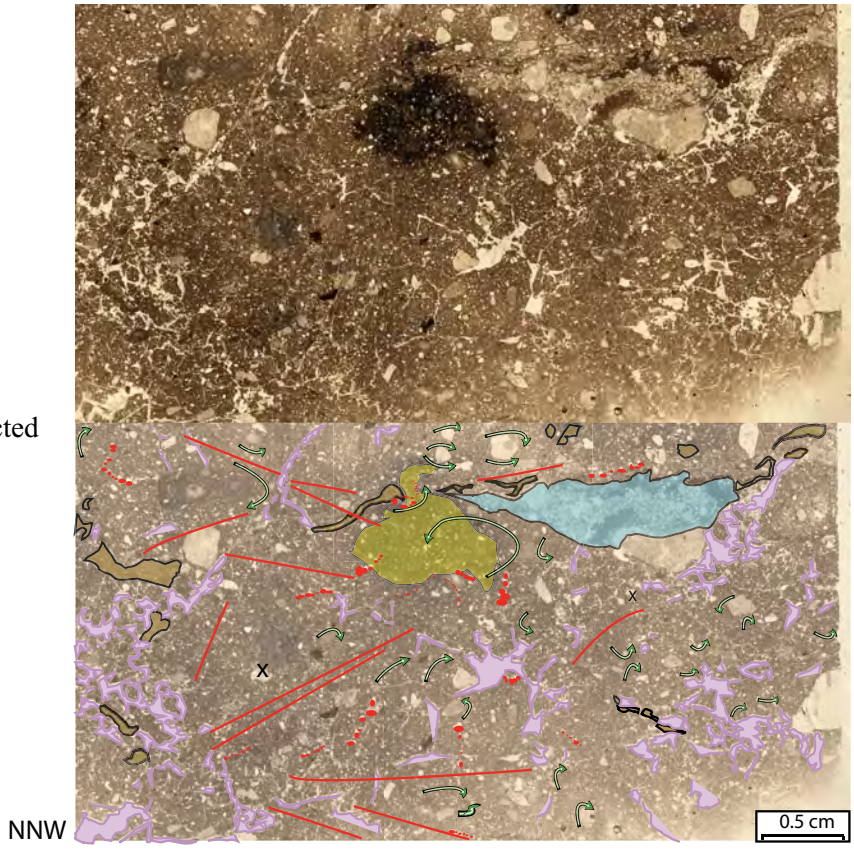

APPENDIX A continued.

Sample 11-PTA-031.
This sample was collected at an azimuth of 040°.

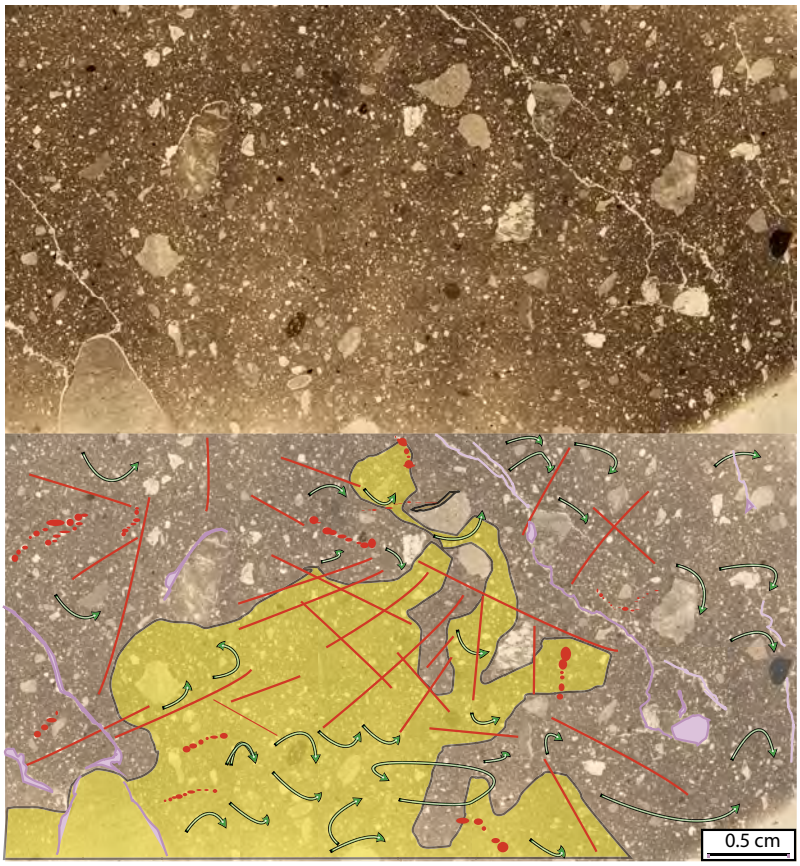

Sample 11-PTA-032.
This sample was collected at an azimuth of 315°.

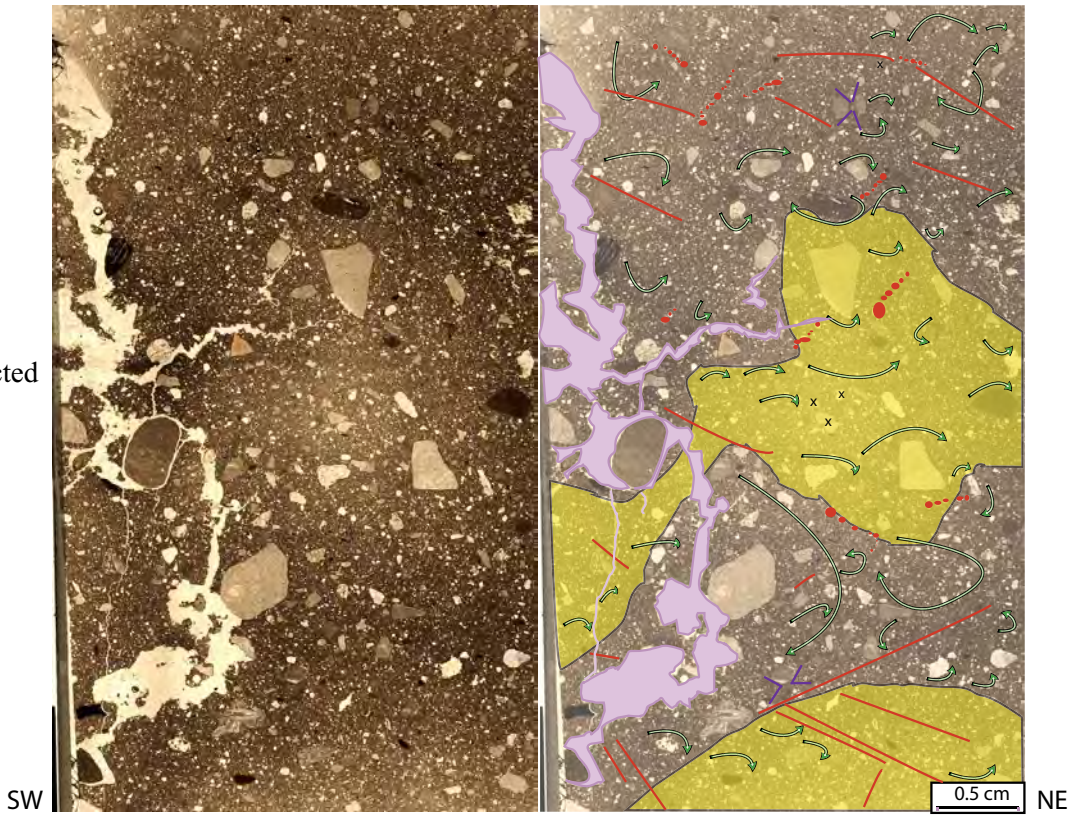

APPENDIX A continued.

Sample 11-PTA-035. This sample was collected at an azimuth of 315°.

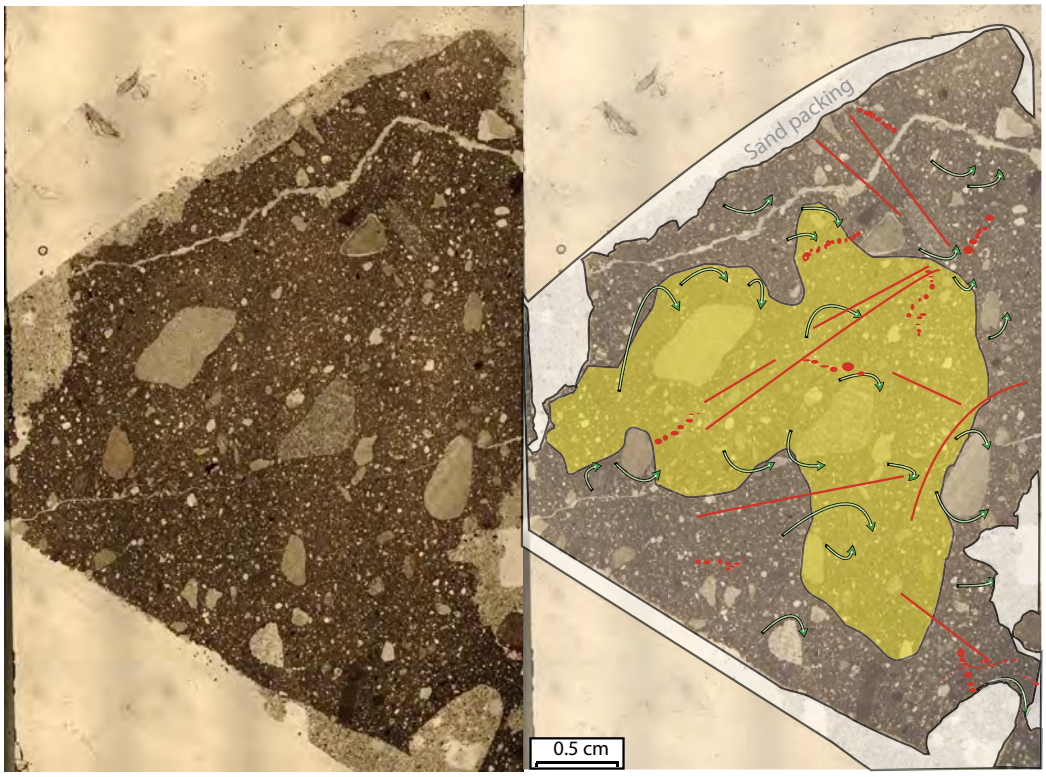

Sample 11-PTA-036. This sample was collected at an azimuth of 315°.

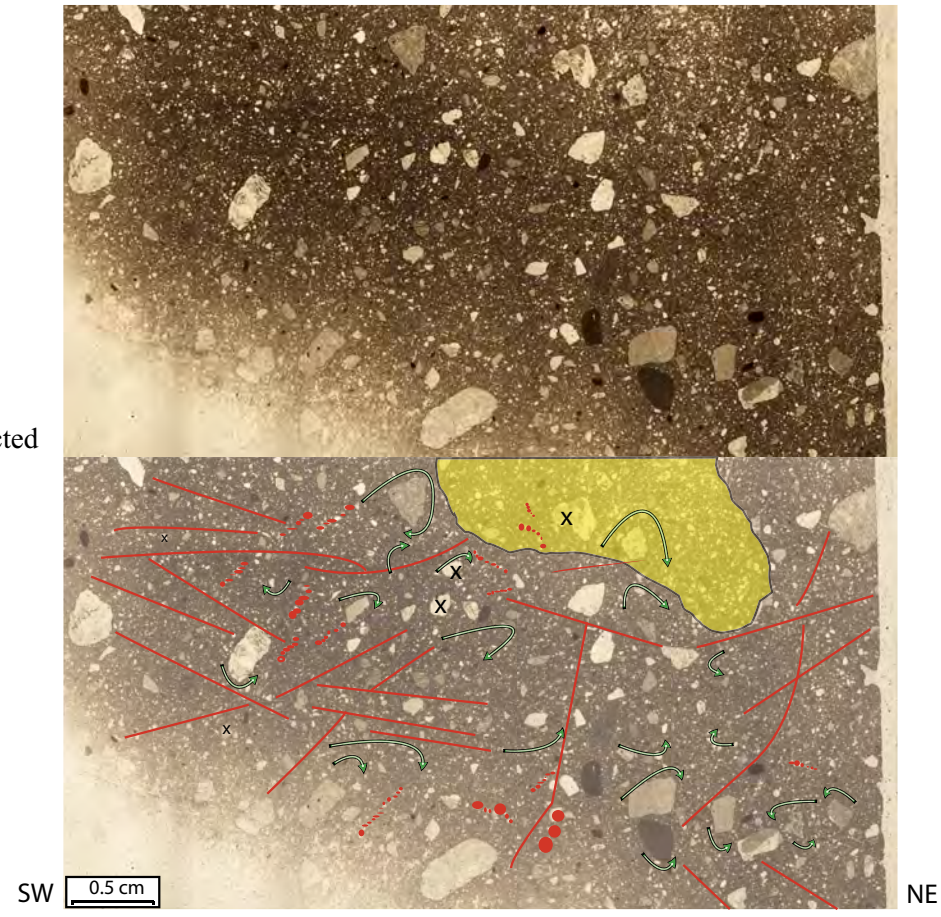

APPENDIX A continued.

Sample 11-PTA-037.
This sample was collected at an azimuth of 315°.

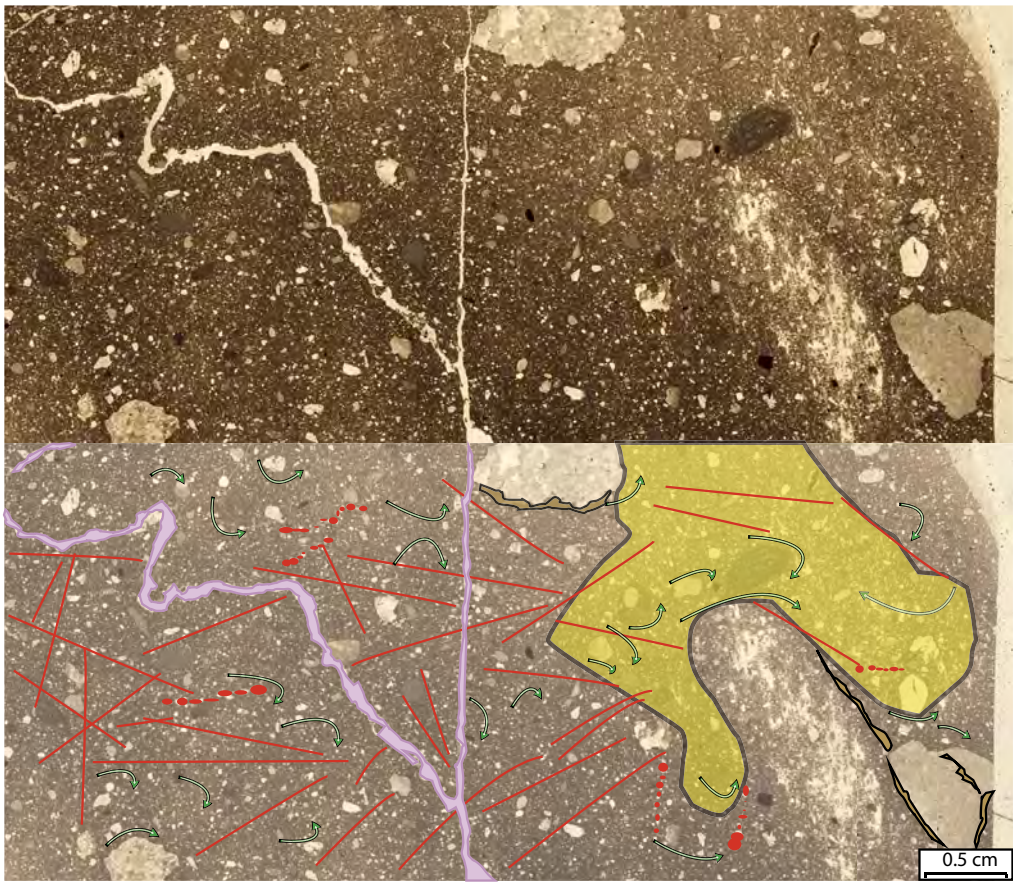

Sample 11-PTA-038.
This sample was collected at an azimuth of 350°.

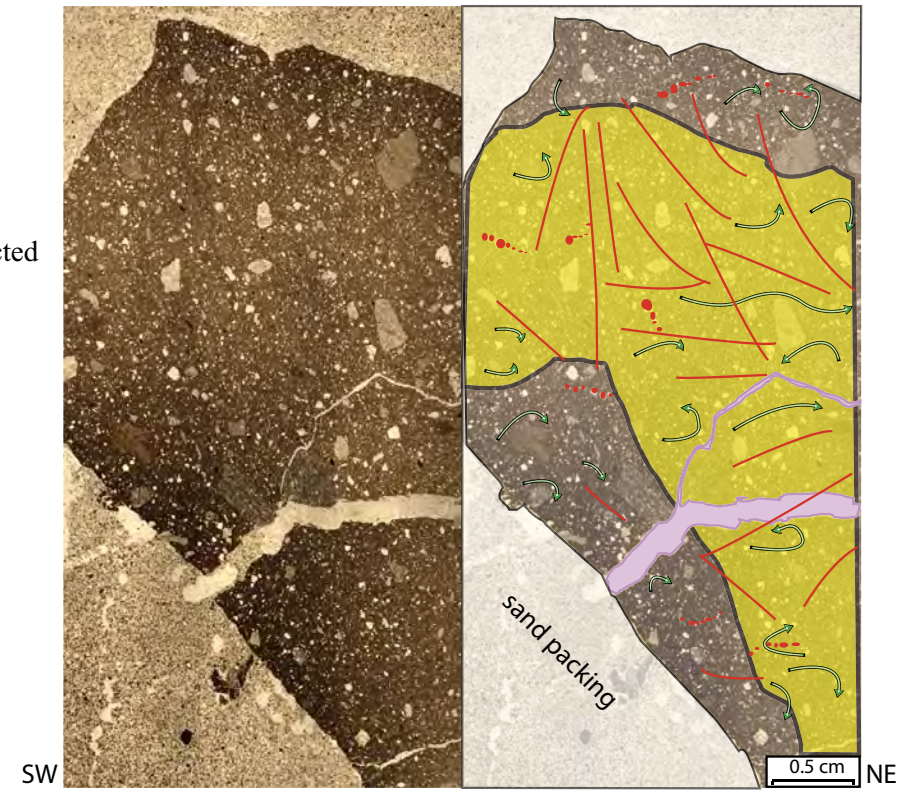

APPENDIX A continued.

Sample 11-PTA-040.
This sample was collected at an azimuth of 330°.

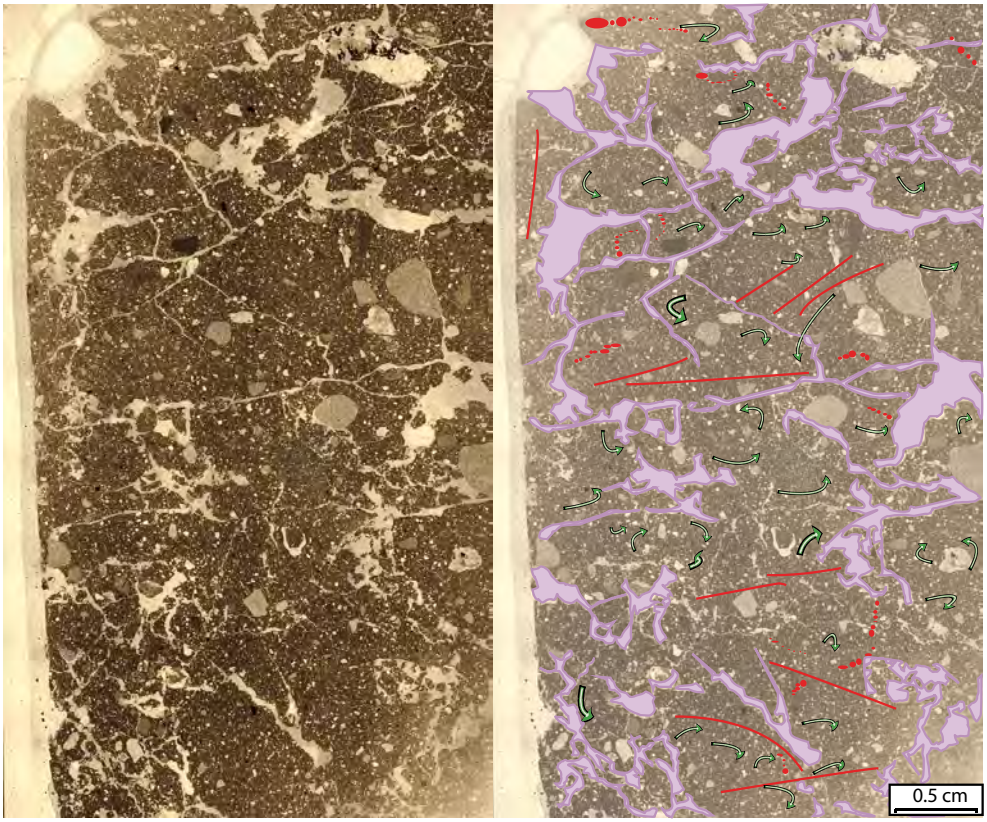

WSW ENE

Sample 11-PTA-041.
This sample was collected at an azimuth of 350°.

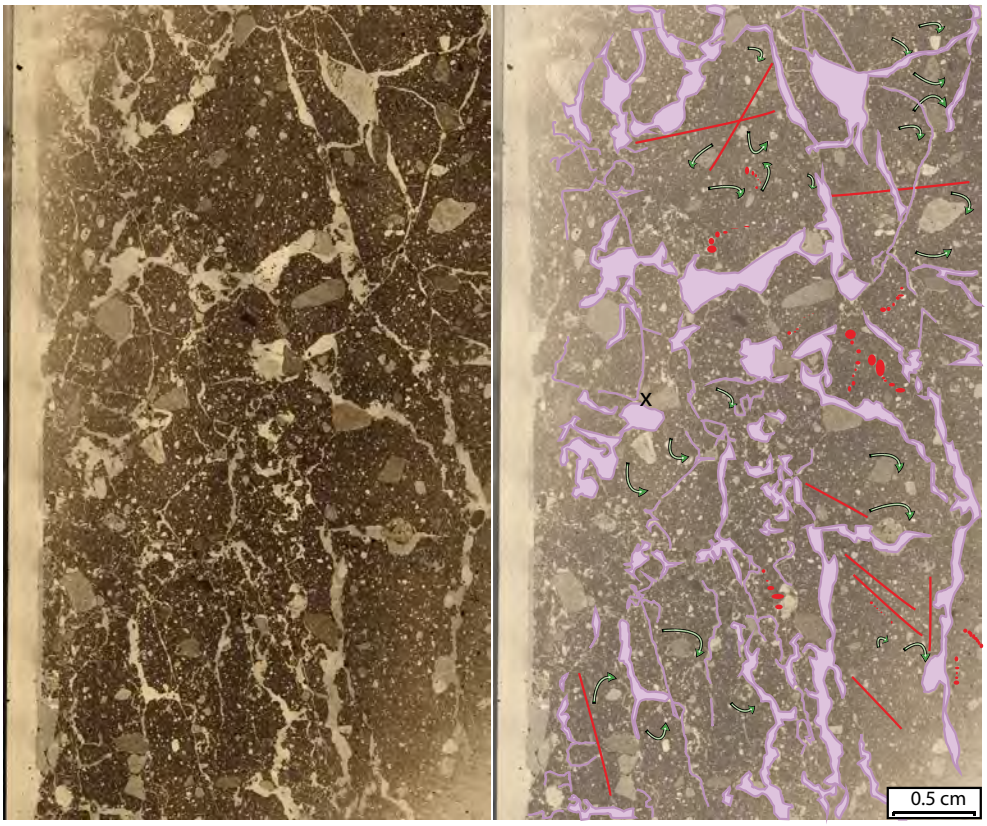

WSW ENE

APPENDIX A continued.

Sample 11-PTA-042.
This sample was collected at an azimuth of 340°.